FLEXURAL BEHAVIOR OF PRESTRESSED CONCRETE MONOBLOCK CROSSTIES

BY

HENRY E. WOLF

THESIS

Submitted in partial fulfillment of the requirements
for the degree of Master of Science in Civil Engineering
in the Graduate College of the
University of Illinois at Urbana-Champaign, 2015

Urbana, Illinois

Advisers:

Research Scientist and Senior Lecturer J. Riley Edwards
Professor David A. Lange

ABSTRACT

The purpose of this research was to improve the current understanding and state of practice for the flexural design and the flexural behavior of prestressed concrete monoblock crossties. Throughout the international railway community, many methods have been developed to analyze the flexural demand of concrete crossties. The current flexural analysis methodologies contained in American Railway Engineering and Maintenance-of-way Association (AREMA) Chapter 30, EuroNorm (EN) 13230, International Union of Railways (UIC) 713R, and Australian Standard (AS) 1085.14 are explained and compared in this thesis. A linear-elastic crosstie analysis model was developed to perform a parametric study to determine the sensitivity of the crosstie to changes in ballast reaction along the crosstie. The results of this parametric study were compared to existing design recommendations to find allowable levels of ballast reaction that can occur beneath the crosstie before crosstie failure is expected. This model was also used to calculate theoretical bending moment values under ballast reactions measured in the field. Based on the results of these analyses, recommendations to improve current design and maintenance practices for prestressed concrete crossties are presented.

To measure the bending moments and support conditions experienced in North American heavy-haul freight service, surface strain gauges were mounted to ten concrete crossties along a high-tonnage, heavy-haul North American freight railroad line. Data were collected from over 7,500 axles from fourteen train passes over three site visits in the spring. The variation of the measured bending moments were found to be non-normally distributed, with a negative skew, indicating a large number of high bending moments experienced by the crosstie. Although minor cracking was observed at the center of most crossties in this test section, measured bending moments and strains did not exceed the current industry standard design limits. Ballast support conditions were found to be a major source of variation in crosstie flexure and were found to be highly variable in both the longitudinal and transverse direction.

Warping or curling due to temperature gradients is a well-documented behavior in concrete pavements, girders, and slab-track, but this behavior has not been documented in concrete crossties. Curling in concrete crossties was investigated using finite element modeling along with data obtained

from laboratory and field experimentation. Curling was found to follow a direct relationship with thermal gradient. Both analytical and empirical methods were found for predicting curl based solely on temperature measurements. Finally, field experimentation was conducted on a North American heavy-haul freight railroad line to investigate the effect temperature-induced curl has on center negative bending moments. The results from data obtained during three separate site visits show a strong inverse relationship between temperature gradient and center negative bending moments.

To my parents,

for loving and teaching me.

To Jesus,

my strength and salvation.

Philippians 4:13

ACKNOWLEDGEMENTS

Rail Product Solutions (RPS), Inc. (formerly Amsted RPS), the National University Rail (NURail) Center (a US DOT-OST Tier 1 University Transportation Center), the Federal Railroad Administration (FRA), and the Union Pacific Railroad have all supported my education and research during my graduate studies and to them I am forever grateful.

I would like to thank the many members of the railroad industry that took an interest in me and my work, and for all of the support they provided. Thank you to John Bosshart, Rusty Croley, Erik Frohberg, Mauricio Gutierrez, Ryan Kernes, Pedro Lemmertz, Mike McHenry, Vince Petersen, Ryan Rolfe, and Cam Stuart for their feedback and contribution in AREMA Committee 30 (Ties) meetings. Special thanks are in order for Steve Mattson (a co-author of a paper in which text was used for significant portions of parts of Chapters 1 & 2) and Arnold Pieringer for their collaboration in the development of the AREMA Chapter 30, Section 4.4 proposal. Thank you to Antonio Buelna, Doug Mroczek, and Chris Roop for their support in laboratory and field testing.

Thanks are due to the all the wonderful students, faculty, and staff in RailTEC. Thank you to the many hourly assistants who helped with this work, including Max Silva, Quinn Todzo, Tom Roadcap, Phanuwat Kaewpanya, and Zhipeng Zhang. Thank you to the graduate research assistants Thiago Bizzarria do Carmo, Sam Chadwick, Zhe Chen, Aaron Cook, Garrett Fullerton, Arkaprabha Ghosh, Matt Greve, Xiao Lin, Andrew Scheppe, Marcelo Suarez, Haichuan Tang, Sihang Wei, Brandon Wang, and Brent Williams. Special thanks to Josué Cesar Bastos, Zhengboyang Gao, Donovan Holder, and Kaijun Zhu for being constant sources of friendship, support, and inspiration. Also, thank you to Matt Csenge and Yu Qian for the thousands of miles of travel, the hours of lab and field work, and the many times you picked me up in tough times on the road. Thank you to Professor David Lange for your contagious enthusiasm and forward-thinking mindset.

I would also like to express my sincerest thanks to Riley Edwards and Marcus Dersch for providing professional and spiritual mentoring during my time as a graduate studies. Both were tremendous in my development as an engineer, researcher, and person. Thank you Riley for introducing

me to research, investing significant time and energy into building my faith, pushing me to utilize my strengths, and encouraging me in my growth areas. Thank you Marcus for helping me to prioritize tasks, teaching me the value of listening, providing insightful and thoughtful feedback, and exemplifying a life focused on the things that matter most.

Finally, thank you to my friends and family. To Zach Boehmke, Brendan McDonnell, Adam Sukiennik, and the Illinois Cross Country and Track Clubs, thank you for forcing me to take breaks and have fun, giving me a life outside of this work. To my brothers, William and Robert, thank you for your friendship and encouragement. To my parents, Richard and Ava, words cannot begin to capture my thanks. Thank you for your unconditional love, your unwavering support, and your sacrificial commitment to help me in any way possible.

TABLE OF CONTENTS

CHAPTER 1: INTRODUCTION[1]

1.1. Purpose

The purpose of this research was to improve the current understanding and state of practice for the flexural design and the flexural behavior of prestressed concrete monoblock crossties.

1.2. Prestressed Concrete Crossties

The majority of the railroad track in North America is supported by ballast (Anon. 2008). A ballasted track system typically consists of rail, fastening systems, crossties, ballast, sub-ballast, and subgrade. The primary purpose of the crosstie is to maintain track geometry (e.g. gauge, cross level, etc.) and to transfer applied wheel loads to the track substructure. The most common material used for crossties in North America is timber, making up 90-95% of crossties in revenue service (Anon. 2008). Concrete is the second most commonly used material, making up most of the remaining 5-10%. Steel and composite crossties are also used, but they make up a negligible share of the total number of crossties in service.

Concrete crossties were first used in the United States in 1893. These early crossties were reinforced with steel and experienced cracking and deterioration failures, causing most to be removed from track within the first few years of their service (Hay 1982). Worldwide, there were scattered trials of concrete crossties during the early 1900's, but a concentrated investigation into concrete crossties was not necessitated until the wake of World War II when Europe experienced a scarcity in timber (Hay 1982).

1.2.1. Monoblock vs. Twin-block Crossties

Early on, two alternative concrete crosstie designs emerged, the monoblock and twin-block crosstie. The monoblock crosstie is more similar to a traditional timber crosstie, with a prismatic shape and a single material continuously extending the length of the member. Traditionally, concrete monoblock crossties have varying sectional properties along the length of the member with larger sections (higher moment of inertia) near the rail seat tapering to smaller sections (lower moment of inertia) at the center. Twin-block

[1]Much of Chapter 1 was originally published in Proceedings of the 2015 International Heavy Haul Association Conference in Perth, AU (Wolf et al. 2015)

crossties feature two concrete blocks at each rail seat linked together with a steel section at the center. Currently, monoblock crossties are commonly used in many countries, including the United States, the United Kingdom, Germany, and Australia. Twin-block crossties are not as common worldwide, and are most commonly used in France and Belgium (FIP 1987). Because there is no concrete center section for twin-block crossties, center negative cracking is not a concern.

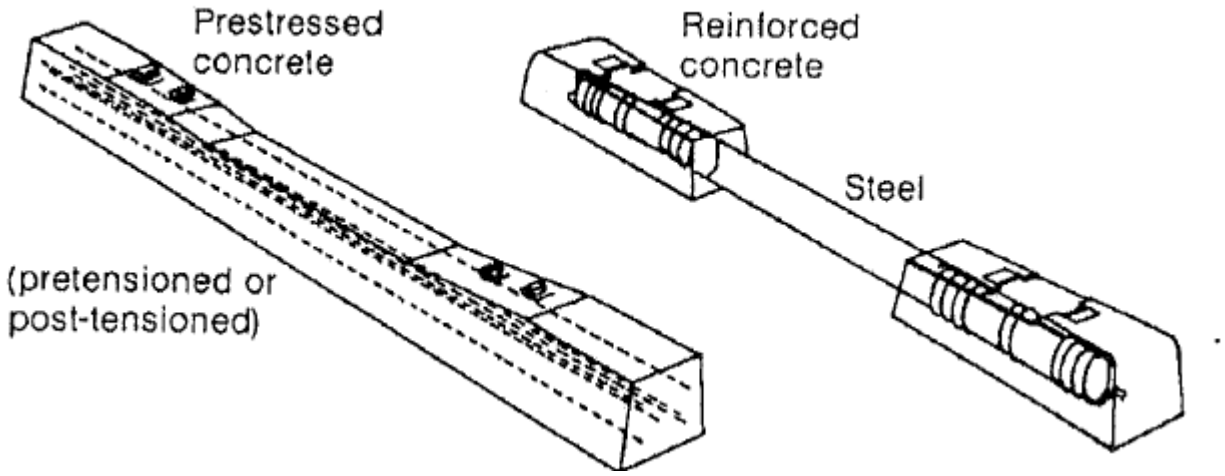

Figure 1.1 Monoblock and twin-block concrete crossties (from FIP 1987)

1.2.2. Prestressed concrete

Monoblock (and sometimes twin-block) concrete crossties are typically prestressed. Prestressing is a process that holds concrete in compression using tensioned steel. This can be achieved by tensioning steel wires or strands before or after the concrete is cast (Nawy 2003). Members made this way are referred to as "pretensioned" and "post-tensioned", respectively (Nawy 2003). Prestressing significantly increases concrete's flexural strength, ductility, and resistance to cracking. Because of these structural improvements, a compelling argument could be made that the success seen in concrete crossties is owed in large part to advances in prestressing theory and technology made between 1870 and 1950.

Early concepts of prestressed concrete were patented in 1872 by P.H. Jackson (Nawy 2003). This idea involved lashing individual blocks together with a tensioned tie rod (Nawy 2003). C.W. Doehring took prestressed concrete a step further in 1888 when he patented a technique of prestressing concrete

slabs with pre-tensioned metal wires (Nawy 2003). These techniques were hampered by struggles of prestress loss in the section, effectively reducing the material to non-prestressed reinforced concrete (Nawy 2003). Eugene Freyssinet was the next major advancer of prestressed concrete. From 1926 to 1928, Freyssinet developed methods that reduced the loss in prestress through the use of high-strength, high-ductility steel (Nawy 2003). With the end of World War II, T.Y. Lin and others developed design techniques for prestressed concrete that are still used today (Nawy 2003). By the early 1960's, it was common practice for monoblock crossties to be prestressed (Hay 1982, FIP 1987, Zeman 2010). Pretensioning in either long-line or carousel systems is the more common practice in the manufacture of monoblock crossties today. For the reasons described above, the prestressed concrete monoblock crosstie emerged as the most common type of concrete crosstie in North America, and will be the focus of this thesis.

1.3. Motivation and Objectives

As the demands placed on infrastructure used by freight and passenger trains increase, it is critical that the performance of the track infrastructure advances to meet these demands. Much research has been performed to quantify the flow of forces in railroad track, but there is still a limited understanding of the complex behavior of concrete crosstie track. Currently, in North America, a largely empirical approach is employed in the design of track components (Van Dyk 2013). This empirical design approach often neglects an analytical understanding in favor of practical experience. One critical track component that is designed using this empirical approach is the crosstie.

Researchers at the University of Illinois-Urbana/Champaign (UIUC) have recently conducted two surveys to assess the most critical issues in concrete crosstie track. The first survey polled 19 individuals at six major (Class I) railroads, two regional and shortline railroads, and four commuter agencies and transit authorities (Zeman 2010). Respondents were asked to rank eight common track problems in concrete crosstie track, with 8 being the most critical and 1 being least. The results from the twelve respondents from Class I railroads are given below.

Table 1.1 Most critical problems in concrete crosstie track (Zeman 2010)

Most Critical Concrete Tie Problems	Average Rank
Rail seat deterioration (RSD)	6.83
Shoulder/fastener wear or fatigue	6.67
Derailment damage	4.83
Cracking from center binding	4.58
Cracking from dynamic loads	1.83
Tamping damage	1.83
Other (ex. manufactured defect)	1.33
Cracking from environmental or chemical degradation	1.25

In the comments section of the survey, Class I respondents reported "tie breakage" and regional/shortline respondents mentioned low prestress leading to rail seat positive bending failure (Zeman 2010).

To gain more perspective on critical concrete crosstie issues, a second survey was conducted in 2013, hereby called the "International Survey". The International Survey was distributed to railroad professionals across four continents (Asia, Australia, Europe, and North America) (Van Dyk 2013). Respondents represented the wide spectrum of interests and knowledge involved in railroad infrastructure, including railroad employees, academic researchers, and component manufacturers. Among its many questions, the International Survey also asked respondents to rank eight common problems in concrete crosstie track. Again, for ranking, 8 was the most critical and 1 was the least critical. The overall ranking for international respondents is listed in parenthesis.

Table 1.2 Most critical problems in concrete crosstie track (Van Dyk 2013)

Most Critical Concrete Tie Problems	Average Rank (North America)	Average Rank (International)
Deterioration of concrete material beneath the rail	6.43	3.15 (8)
Shoulder/fastening system wear or fatigue	6.38	5.50 (2)
Cracking from dynamic loads	4.83	5.21 (4)
Derailment damage	4.57	4.57 (6)
Cracking from center binding	4.50	5.36 (3)
Tamping damage	4.14	6.14 (1)
Other (ex. manufactured defect)	3.57	4.09 (7)
Cracking from environmental or chemical degradation	3.50	4.67 (5)

From both surveys it is clear that RSD, shoulder/fastening system wear, derailment damage, and crosstie cracking (center binding and dynamic loads) are all critical issues in concrete crosstie track. Much research has been conducted at UIUC focused on RSD and fastening system damage (Zeman 2010, Kernes 2011, do Carmo 2014, Greve 2015). This work has led to several updates and improvements to the American Maintenance and Right-of-way Association (AREMA) Manual for Railway Engineering (MRE), considered the primary source for recommended practices for track structure and component design in North America (AREMA 2014). Less investigation has gone into crosstie flexure, the cause of concrete cracking due to center binding and dynamic loads (Zeman 2010, Chen 2014, Wei 2014). As of 2014, none of this work has translated into changes into AREMA recommendations. For these reasons, it was deemed necessary to further investigate crosstie flexure in attempt to improve the understanding and state of practice of the flexural behavior of prestressed concrete monoblock crossties.

1.4. Flexural Analysis and Design Methodologies

In order to improve the flexural performance of concrete crossties, it was necessary to first understand the current practices used in the structural design of these members. The structural design process consists of two steps. First, an *analysis* is performed to estimate the demand (i.e. flexure, shear, etc.) that a structural element is expected to undergo in its lifetime. Second, the element is *designed* to meet or exceed the demand found in the analysis. Currently, design standards produced by organizations such as AREMA (2014), EuroNorm (EN) (2009), International Union of Railways (UIC) (2004), and Australian Standard (AS) (2003) only provide formal recommendations on the analysis portion of the structural design process. In this section, an explanation and comparison of the analysis methodologies proposed by AREMA, EN, UIC, and AS will be provided.

1.4.1. American Railway Engineering and Maintenance-of-way Association (AREMA C30)

The 2015 AREMA method for concrete crosstie flexural analysis is a factored approach that is dependent on crosstie length, crosstie spacing, annual tonnage, and train speed. Design bending moments are given for four key locations on the crosstie: rail seat positive (M_{RS+}), rail seat negative (M_{RS-}), center positive (M_{C+}), and center negative (M_{C-}). To begin, AREMA Figure 30-4-3 is used to determine the factored

design bending moment for a given loading condition. By specifying the crosstie spacing and the crosstie length, an unfactored rail seat positive bending moment (B) can be found from AREMA Figure 30-4-3. AREMA Figure 30-4-4 is then used to determine the speed (V) and tonnage factors (T), which are based on expected track speed and tonnage, respectively. These three values are multiplied together using Equation 1.1. For each figure, linear interpolation can be performed between two specified points to obtain a more accurate factor.

$$M_{RS+} = B \times V \times T \tag{1.1}$$

where, M_{RS+} = factored rail seat positive bending moment (kip-in (kNm))

B = unfactored rail seat positive bending moment (kip-in (kNm))

V = speed factor

T = tonnage factor

Once the design rail seat positive bending moment is determined, it is multiplied by other factors to determine design bending moments at the three other key locations. The factors are based on crosstie length and can be linearly interpolated (AREMA Table 30-4-1).

The origins of AREMA Figure 30-4-3 are unclear, but a paper by McQueen (1983) suggests that the chart is based on an 8'-6" (2.6 m) crosstie with 60" (1524 mm) rail center-to-center spacing under an 82 kip (365 kN) axle load, as pictured in **Figure 1.2a**. The ballast reaction is assumed to be uniform along the entire length of the crosstie.

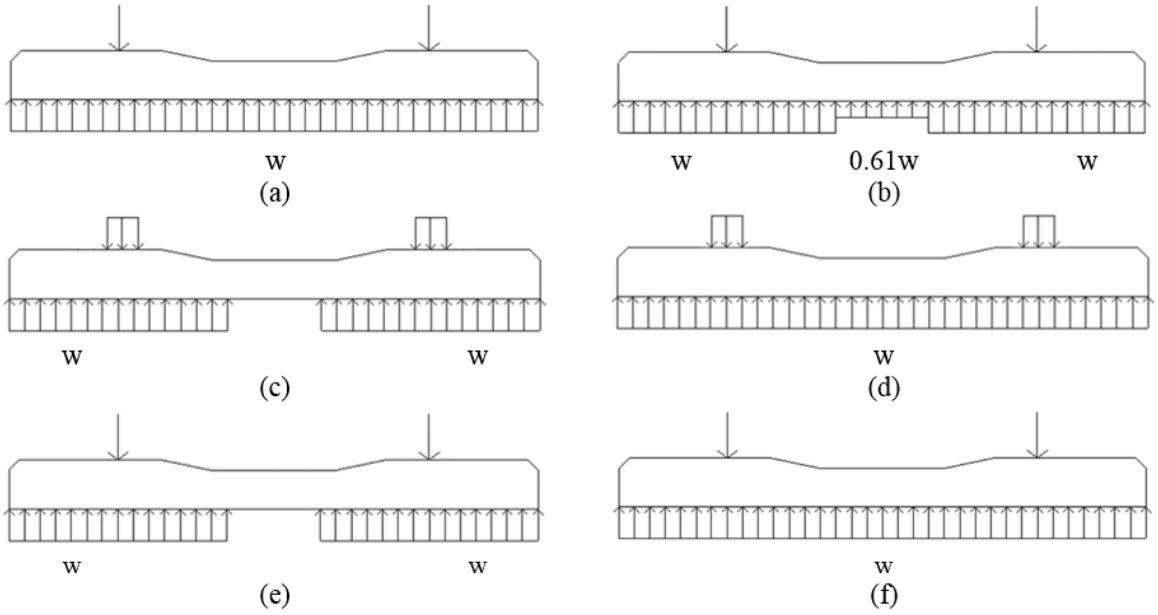

Figure 1.2 Support conditions for select design recommendations:
(a) AREMA M_{RS+}, (b) AREMA M_{C-}, (c) UIC M_{RS+}, (d) UIC M_{C-}, (e) AS M_{RS+}, (f) AS M_{C-}

The rail seat load is computed according to the AREMA recommendation, using Equation 1.2 below.

$$R = WL \times DF \times (1 + IF) \tag{1.2}$$

where, R = design rail seat load (kip (kN))

WL = unfactored wheel load (kip (kN))

DF = distribution factor (from AREMA Figure 30-4-1)

IF = impact factor (specified to be 200% by AREMA)

Thus, for an 82 kip (365 kN) axle load, 24" (610 mm) crosstie spacing, and 200% impact factor, the design rail seat load is 62.1 kips (276.2 kN).

Because the ballast reaction is assumed to be uniform along the entire crosstie, the reaction can be found by multiplying the design rail seat load by two (to account for both rail seats) and then dividing by the length of the crosstie. So, for an 8'-6" (2.6 m) crosstie with a design rail seat load of 62.1 kips (276.2 kN), the distributed ballast reaction is 1.22 kips/in (213 kN/m). McQueen then calculates the rail seat

bending moment by modeling the end of the crosstie to the design rail seat load as a cantilever, using Equation 1.3 below.

$$M = \frac{wc^2}{2} \tag{1.3}$$

where, M = unfactored rail seat positive bending moment (kip-in)

w = distributed ballast reaction (kips/in)

c = cantilever length (in)

McQueen then applies a 10% factor to account for prestress losses. Most concrete crosstie manufacturers consider prestress losses in their design, meaning this increase of 10% is essentially a safety factor. After this factor is applied, the product is rounded up to the nearest 5 kip-in to get the design rail seat positive bending moment. By applying this safety factor and rounding, the design rail seat positive bending moment proposed by McQueen is 300 kip-in (33.9 kNm). This value matches the bending moment value given by AREMA Figure 30-4-3 for an 8'-6" (2.6 m) crosstie at 24" (610 mm) spacing.

This design rail seat positive bending moment is then multiplied by factors in AREMA Table 30-4-1 to find values for design bending moments at the other critical regions. For an 8'-6" (2.6 m) crosstie AREMA specifies a factor of 0.67 to calculate center negative bending moment. Thus, using the 300 kip-in (33.9 kNm) rail seat positive bending moment, the center negative bending moment is 201 kip-in (22.7 kNm). For an 8'-6" (2.6 m) crosstie with 60" (1524 mm) rail center-to-center spacing, this center negative bending moment can be found when the reaction at an 18" (457 mm) center section is reduced 39% (**Figure 1.2b**). These support conditions were found considering the 10% safety factor. It is also important to remember that these design bending moments values would then be multiplied by a tonnage and train speed factor, which could increase the values by as much as 32% (factor of 1.32).

1.4.2. EuroNorm (EN 13230-1) / International Union of Railways (UIC 713R)

EN 13230-1 states that the purchaser must specify the design bending moments to the crosstie manufacturer. In Annex E, it defers the analysis of design bending moments to UIC 713R. The 2004 UIC 713R method of analysis is dependent on crosstie length, crosstie spacing, axle load, rail pad attenuation,

and train speed. Like AREMA, UIC also provides a pair of safety factors, one to account for "variation in crosstie reaction due to support faults" and another to account for "irregularity in the support along the crosstie."

As seen previously in McQueen's method, the design rail seat load must first be calculated in order to perform the flexural analysis of the crosstie. The crosstie is assumed to be under a "newly tamped" condition, with the ballast reaction occurring symmetrically about the rail seat load (**Figure 1.2c**). Equation 1.4 below is used to calculate the design rail seat load according to UIC 713R.

$$R = \frac{Q_0}{2}(1 + \gamma_p\gamma_v)\gamma_d\gamma_r\gamma_i \tag{1.4}$$

where, R = design rail seat load (kip)

Q_0 = unfactored axle load (kip (kN))

γ_p = rail pad attenuation factor (UIC 713R recommends 1.0 for low attenuation)

γ_v = speed factor (UIC 713R recommends 0.5 for speeds under 125 mph (200 km/hr))

γ_d = distribution factor (UIC 713R recommends 0.5 for crosstie spacing under 25.6" (650 mm))

γ_r = reaction support fault safety factor (UIC 713R recommends 1.35)

γ_i = support irregularity safety factor (UIC 713R recommends 1.6)

Thus, for an 82 kip (365 kN) unfactored axle load and the UIC 713R-recommended factors, the design rail seat load found according to UIC 713R is 66.4 kips (295.4 kN), or 7% greater than the AREMA recommendation.

Next, UIC 713R calculates the rail seat positive bending moment for the crosstie with Equation 1.5.

$$M_{RS+} = \frac{R}{4}\left(c - \frac{f}{2} - \frac{h}{2}\right) \tag{1.5}$$

where, M_{RS+} = design rail seat positive bending moment (kip-in (kNm))

R = design rail seat load (kip (kN))

c = cantilever arm (kip (kN))

f = width of rail base (in (mm))

h = depth of crosstie (in (mm))

There are several assumptions made in this equation. First, the rail seat load is assumed to be uniformly distributed over the entire width of the rail seat. As seen in research conducted at the University of Illinois at Urbana-Champaign (UIUC), this assumption is not necessarily valid, especially in the presence of lateral loads and high lateral to vertical (L/V) load ratios (Greve 2014). The distributed rail seat load causes the moment at the center of the rail seat to be reduced, which is explained in further detail by Freudenstein (2007). Additionally, UIC 713R assumes that the crosstie behaves as a deep beam, transferring the rail seat load in a compressive field spreading at a 45-degree angle to the neutral axis of the crosstie (assumed in the above equation to be one-half of the crosstie height). This means that for a 9" (229 mm) deep crosstie supporting a rail seat 6" (152 mm) wide, the rail seat load is distributed over a length of 15" (381 mm). This causes a significant reduction in moment. Thus, for a crosstie of length of 8'-6" (2.6 m), depth of 9" (229 mm), and rail center-to-center spacing of 60" (1524 mm), under an 82 kip (365 kN) unfactored axle load on 6" (152 mm) rail seats the design rail seat positive bending moment per UIC 713R is 224 kip-in (25.3 kNm), a 25% reduction from the AREMA recommendation.

UIC 713R calculates the center negative bending moment using three methods. First, Equation 1.6 can be used for a crosstie with constant width. Two alternative equations can be used for crossties with waisted (i.e. narrow) center sections, both of which account for a reduction in the center negative bending moment.

$$M_{C-} = \frac{R}{2}\left(g - \frac{2L^2 - b^2}{2(2L - b)}\right) \tag{1.6}$$

where, M_{C-} = design center negative bending moment (kip-in (kNm))

R = design rail seat load (kip (kN))

g = rail center-to-center spacing (in (mm))

L = crosstie length (in (mm))

b = width of reduced center reaction (in (mm))

This equation takes a 50% reduction in center reaction into account with the term "b", as seen in UIC 713R Figure 1, case (b). UIC recommends this "partially consolidated" support condition for constant-width crossties, but ultimately leaves the center reaction reduction to the discretion of the crosstie purchaser. Freudenstein uses the assumption that there is no reduction in the center reaction and that there is a uniform ballast reaction along the entire length of the crosstie (b=0" (0 mm)) as shown in **Figure 1.2d**. The center negative bending moment can be found by modeling the crosstie as a cantilevered beam fixed at the crosstie center with a rail seat load acting downwards and the ballast reaction acting upwards. Thus, for a constant-width crosstie of length 8'-6" (2.6 m) and 60" (1524 mm) rail center-to-center spacing, under an 82 kip (365 kN) unfactored axle load, the design center negative bending moment per UIC 713R is 299 kip-in (33.8 kNm), a nearly 50% increase from the AREMA recommendation. After the design rail seat positive and center negative bending moments are calculated, they are multiplied by factors of 0.5 and 0.7, respectively, to get design rail seat negative and center positive bending moments.

1.4.3. Australian Standard (AS 1085.14)

The 2003 AS method for crosstie flexural analysis is dependent on crosstie length, crosstie spacing, and axle load. As in the previously demonstrated methods, the rail seat load must first be computed. AS 1085.14 proposes an equation that is similar to the AREMA recommendation, seen in Equation 1.7.

$$R = j \times WL \times DF \tag{1.7}$$

where, R = design rail seat load (kip (kN))

j = impact factor (AS 1085.14 states it shall not be less than 2.5)

WL = unfactored wheel load (kip (kN))

DF = distribution factor (from AS1085.14 Figure 4.1)

Thus, assuming the minimum impact factor of 2.5, under an 82 kip (365 kN) axle load and 24" (610 mm) crosstie spacing, the design rail seat load is 53.3 kips (237.2 kN). One difference between this method and AREMA are the magnitudes of the impact and distribution factors. AREMA calls for a 200% impact factor, but this factor is added to 1.0 such that the true impact factor is 3.0, compared to the 2.5 used in AS 1085.14. If AS expressed this impact factor in the same manner as AREMA, it would be 150%. An

impact factor of 150% was used by AREMA in the past, but it was since raised to its current value of 200% (McQueen 2010). Another difference is seen in the distribution factor figures (AREMA Figure 30-4-1 and AS1085.14 Figure 4.1), which give slightly different values, approximately 50.5% and 52% for AREMA and AS, respectively. AS 1085.14 and AREMA C30 both differ from UIC 713R by not including reductions for rail pad attenuation or safety factors to account for support irregularities or voids. UIC 713R also does not consider load distribution from rail to rail seat as rigorously, using a factor of 0.5 if the rail section is heavier than 93 lbs/yd (46 kg/m) and the crosstie spacing is less than 25.6" (650 mm).

To calculate the design rail seat positive bending moment, AS 1085.14 uses the same support conditions as UIC 713R, assuming the "newly tamped" condition shown in **Figure 1.2e**. However, AS 1085.14 treats the rail seat load as a point load and neglects deep beam behavior, which is similar to McQueen's analysis. This assumption also slightly simplifies the calculation, as seen in Equation 1.8.

$$M_{RS+} = \frac{R(L - g)}{8} \tag{1.8}$$

where, M_{RS+} = design rail seat positive bending moment (kip-in (kNm))

R = design rail seat load (kip (kN))

g = rail center-to-center spacing (in (mm))

L = crosstie length (in (mm))

Thus, for a crosstie of length of 8'-6" (2.6 m) and rail center-to-center spacing of 60" (1524 mm), under an 82 kip (365 kN) unfactored axle load, the design rail seat positive bending moment per AS 1085.14 is 280 kip-in (31.6 kNm), a 7% reduction from the AREMA recommendation and a 25% increase from the UIC recommendation.

The AS 1085.14 center negative analysis is similar to the UIC 713R analysis presented earlier. Both assume uniform ballast reaction along the length of the crosstie, but AS treats the rail seat load as a point load (**Figure 1.2f)**. As a result, the AS 1085.14 equation for design center negative bending moment (Equation 1.9), is the same as the UIC 713R equation for design center negative bending moment (Equation 1.6) when there is no center reaction reduction (b=0" (0 mm)).

$$M_{C-} = \frac{R(2g - L)}{4} \quad (1.9)$$

where, M_{C-} = design rail seat positive bending moment (kip-in (kNm))

R = design rail seat load (kip (kN))

g = rail center-to-center spacing (in (mm))

L = crosstie length (in (mm))

Thus, for a crosstie of length 8'-6" (2.6 m) and 60" (1524 mm) rail center-to-center spacing, under an 82 kip (365 kN) unfactored axle load the design center negative bending moment per AS 1085.14 is 240 kip-in (27.1 kNm), a 20% increase from the AREMA recommendation and a 20% reduction from the UIC recommendation.

Table 1.3 provides a comparison of the results found using the different analysis methods explained above. The maximum bending moment found from the analyses for each critical region is highlighted. A model to quickly and easily perform flexural analysis for a crosstie under varying support conditions is needed to further distinguish between these methodologies, and is developed and presented in the next section. **Table 1.4** lists the factors that are explicitly used in the determination or calculation of design bending moments for prestressed concrete monoblock crossties.

Table 1.3 Comparison of flexural analysis methodologies

	AREMA	UIC	AS
Axle Load (Q_0)	82 kips (365 kN)	82 kip (365 kN)s	82 kip (365 kN)s
Crosstie Length (L)	102 " (2.6 m)	102 " (2.6 m)	102 " (2.6 m)
Rail Center-to-Center Spacing (g)	60 " (1524 mm)	60 " (1524 mm)	60 " (1524 mm)
Width of Rail Base (f)	6 " (152 mm)	6 " (152 mm)	6 " (152 mm)
Depth of Crosstie (h)	9 " (229 mm)	9 " (229 mm)	9 " (229 mm)
Crosstie Spacing	24 " (610 mm)	24 " (610 mm)	24 " (610 mm)
Distribution Factor (DF)	50.5% *a*	50% *b*	52% *c*
Impact Factor (IF)	200%	NA	150%
Rail Pad Attenuation Factor (γ_p)	NA	1.0	NA
Speed Factor (V or γ_v)	1.0 *d*	0.5 *e*	NA
Reaction Support Fault Safety Factor (γ_r)	NA	1.35	NA
Support Irregularity Safety Factor (γ_i)	NA	1.6	NA
Design Rail Seat Load (R)	62.1 kips (276.2 kN)	66.4 kips (295.4 kN)	53.3 kips (237.2 kN)
Tonnage Factor (T)	1.0 *f*	NA	NA
Prestress Safety Factor	10%	NA	NA
Rail Seat Positive Moment (M_{RS+})	300 kip-in (33.9 kNm)	224 kip-in (25.3 kNm)	280 kip-in (31.6 kNm)
Rail Seat Negative Moment (M_{RS-})	159 kip-in *g* (18.0 kNm)	112 kip-in *h* (12.7 kNm)	187 kip-in *i* (21.1 kNm)
Center Positive Moment (M_{C+})	141 kip-in *j* (15.9 kNm)	209 kip-in *k* (23.6 kNm)	112 kip-in *l* (12.7 kNm)
Center Negative Moment (M_{C-})	201 kip-in (22.7 kNm)	299 kip-in (33.8 kNm)	240 kip-in (27.1 kNm)

Notes:
a - From AREMA Figure 30-4-3, for 24" (610 mm) crosstie spacing
b - UIC 713R assumes 50% rail seat load distribution for crosstie spacing less than 25.6" (650 mm)
c - From AS 1085.14 Figure 4.1, for 24" (610 mm) crosstie spacing
d - From AREMA Figure 30-4-4, a specific speed was not designated for this calculation. The speed factor is applied for the calculation of design bending moments.
e - UIC 713R designates a speed factor in the calculation of rail seat load of 0.5 for train speeds below 125 mph (200 km/hr)
f - From Figure 30-4-4, a specific tonnage was not designated for this calculation. The tonnage factor is applied for the calculation of design bending moments.
g - Per AREMA C30, $M_{RS-}=0.53xM_{RS+}$
h - Per UIC 713R, $M_{RS-}=0.5xM_{RS+}$
i - Per AS 1085.14, $M_{RS-}=0.67xM_{RS+}$
j - Per AREMA C30, $M_{C+}=0.47xM_{RS+}$
k - Per UIC 713R, $M_{C+}=0.7xM_{C-}$
l - Per AS 1085.14, $M_{C+}=0.05R(L-g)$

Table 1.4 Different parameters used in flexural analysis methodologies

	AREMA	UIC	AS
Axle Load (Q_0)		●	●
Crosstie Length (L)	●	●	●
Rail Center-to-Center Spacing (g)		●	●
Width of Rail Base (f)		●	
Depth of Crosstie (h)		●	
Crosstie Spacing	●	●	●
Distribution Factor (DF)		●	●
Impact Factor (IF)			●
Rail Pad Attenuation Factor (γ_p)		●	
Speed Factor (V or γ_v)	●	●	
Reaction Support Fault Safety Factor (γ_r)		●	
Support Irregularity Safety Factor (γ_i)		●	
Design Rail Seat Load (R)		●	●
Tonnage Factor (T)	●		

CHAPTER 2: SENSITIVITY OF CONCRETE CROSSTIE FLEXURAL BEHAVIOR TO BALLAST SUPPORT CONDITIONS[2]

2.1. Purpose

The purpose of this research was to investigate the sensitivity of concrete crossties to ballast support conditions. This chapter picks up where **Chapter 1** left off, and uses bending moment values found previously.

2.2. Development of Linear-Elastic Crosstie Analysis Model

To better understand the effect of changing support conditions on crosstie bending moments, it was necessary to develop an analytical model. The authors desired to create a model that was easily accessible and simple to use. As such, Microsoft Excel was chosen as the platform for this tool and basic Euler-Bernoulli beam theory was used.

To further simplify the analysis, half of the crosstie was modeled as a linear-elastic cantilevered beam. This assumed that the crosstie was symmetrically loaded and supported about the center, and that the loading was quasi-static. The ballast reaction was modeled as a distributed load and the rail seat load was modeled as a point load (as seen in the AREMA and AS analyses). This model was developed for a crosstie with a length of 8'-6" (2.6 m) and rail center-to-center spacing of 60" (1524 mm), but can accommodate varying crosstie lengths and rail center-to-center spacings.

In order to quickly adjust the ballast reaction, the reaction was split into sections or "bins". These bins were placed symmetrically about the rail seat load in order to easily simulate different theoretical and experimental ballast reactions. Dividing the rail seat-supported section into six bins was deemed to provide adequate resolution. For an 8'-6" (2.6 m) crosstie, this meant that each rail seat bin was 7" (178 mm). This left a 9" (229 mm) section at the crosstie center, which was split into three bins for consistency

[2] Much of Chapter 2 was originally published in Proceedings of the 2015 International Heavy Haul Association Conference in Perth, AU (Wolf et al. 2015)

and to provide greater resolution at the region expected to be most critical to the center bending moment. **Figure 2.1** shows the set-up of this crosstie model with the ballast reaction split into nine bins.

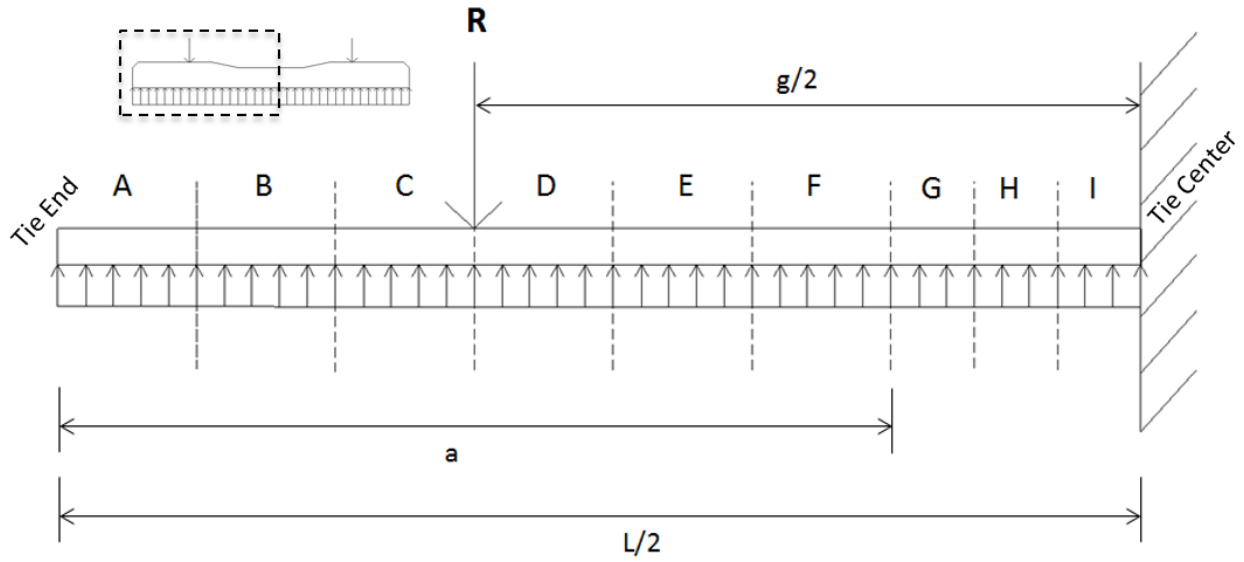

Figure 2.1 Illustration of linear-elastic crosstie model

2.3. Effect of Support Conditions on Crosstie Bending Moments

The goal of the parametric study was to determine the bending moment values that could be experienced by a crosstie under a given rail seat load and different support conditions. First, this problem was bounded by idealizing the ballast reaction as a point load that varies with "x" along the length of the crosstie, as given in Equation 2.1. This idealization assumes that the entire rail seat load is taken by a single discrete point underneath the crosstie. It would be similar to a crosstie being supported symmetrically about the center by two pieces of ballast.

$$M_C = -R\left(\frac{g}{2}\right) + Px \tag{2.1}$$

where, M_C = bending moment at crosstie center (kip-in (kNm))

g = rail center-to-center spacing (in (mm))

R = design rail seat load (kip (kN))

P = ballast reaction (kip (kN))

x = location of ballast reaction

For a rail seat load of 62.1 kips (276.2 kN) on a crosstie with length of 8'-6" (2.6 m) and a rail center-to-center spacing of 60" (1524 mm), the theoretical bending moment extremes at the crosstie center could range from 1,304 kip-in (147.3 kNm) to -1,863 kip-in (-210.5 kNm), where the maximum positive moment occurs when the reaction load occurs at the end of the crosstie and the maximum negative moment occurs when the reaction load occurs at the center of the crosstie. These values are the upper and lower limits of bending moments that could be experienced by the crosstie. However, this method is overly simplified and does not provide realistic support conditions.

To more realistically express the ballast reactions seen in track, the percentage of total reaction taken by each bin was modified. To compare the sensitivity of the reaction of each bin on the bending moments, each bin was modified separately, such that the ballast reaction in one bin changed and the ballast reactions in the other eight bins shared the remainder of the reaction equally. For example, if bin A takes 0% of the rail seat load, 100% of the ballast reaction would be shared equally between bins B-I. The rail seat and center bending moments under these conditions are found to be 138 kip-in (15.6 kNm) and -497 kip-in (-56.2 kNm), respectively. Similarly, if bin C takes 25% of the rail seat load, the remaining 75% is split equally to bins A, B, and D-I, for a rail seat moment of 262 kip-in (29.6 kNm) and a center moment of -215 kip-in (-24.3 kNm). The complete results of this study are shown in **Table 2.1**. The rail seat load used in these analyses was 62.1 kips (276.2 kN).

Table 2.1 Effect of ballast reaction on M_{RS} and M_C

Section		A	B	C	D	E	F	G	H	I
Rail Seat Moment (M_{RS}) kip-in (kNm)	0%	138 (15.6)	207 (23.4)	277 (31.3)	311 (35.1)	311 (35.1)	311 (35.1)	285 (32.2)	285 (32.2)	285 (32.2)
	25%	375 (42.4)	319 (36)	262 (29.6)	233 (26.3)	233 (26.3)	233 (26.3)	214 (24.2)	214 (24.2)	214 (24.2)
	50%	613 (69.3)	430 (48.6)	247 (27.9)	156 (17.6)	156 (17.6)	156 (17.6)	143 (16.2)	143 (16.2)	143 (16.2)
	75%	850 (96)	541 (61.1)	232 (26.2)	78 (8.8)	78 (8.8)	78 (8.8)	71 (8)	71 (8)	71 (8)
	100%	1087 (122.8)	652 (73.7)	217 (24.5)	0 (0)	0 (0)	0 (0)	0 (0)	0 (0)	0 (0)
Center Moment (M_C) kip-in (kNm)	0%	-497 (-56.2)	-428 (-48.4)	-358 (-40.4)	-289 (-32.7)	-220 (-24.9)	-151 (-17.1)	-210 (-23.7)	-198 (-22.4)	-187 (-21.1)
	25%	-101 (-11.4)	-158 (-17.9)	-215 (-24.3)	-272 (-30.7)	-328 (-37.1)	-385 (-43.5)	-506 (-57.2)	-544 (-61.5)	-582 (-65.8)
	50%	295 (33.3)	113 (12.8)	-70 (-7.9)	-253 (-28.6)	-436 (-49.3)	-618 (-69.8)	-804 (-90.8)	-891 (-100.7)	-978 (-110.5)
	75%	691 (78.1)	382 (43.2)	74 (8.4)	-235 (-26.6)	-544 (-61.5)	-853 (-96.4)	-1100 (-124.3)	-1237 (-139.8)	-1374 (-155.2)
	100%	1087 (122.8)	652 (73.7)	217 (24.5)	-217 (-24.5)	-652 (-73.7)	-1087 (-122.8)	-1397 (-157.8)	-1584 (-179)	-1770 (-200)

From the above table, one can see how the shift in the ballast reaction affects the rail seat and center bending moments (**Table 2.1**). As larger percentages of the ballast reaction are taken by bins closer to the crosstie end (A, B), the rail seat and center bending moments both increase, and vice versa. Shaded cells represent moments that exceed the maximum values found using any of the analysis methods explained previously (**Table 1.1)**. It is seen that the rail seat bending moment is always positive and is very sensitive to changes in bins A, B, and C (i.e. the distance between the rail seat and the end of the crosstie). This is seen in the high bending moments when the ballast reaction is concentrated at these bins. As discussed earlier, the magnitude of the center bending moment can be high for either positive or negative bending. The center experiences its maximum positive bending moments when the ballast reaction is concentrated outside of the rail center-to-center spacing and experiences its maximum negative bending moments when the ballast reaction is concentrated inside of the rail center-to-center spacing.

One of the simplest ways to see the sensitivity of a bin is to compare the difference between moments found when the bin takes 0% and 100% of the ballast reaction. For the rail seat bending moment, the most sensitive bin is found to be bin A, where the difference between the moment when 100% of the ballast reaction occurs in bin A (1,087 kip-in (122.8 kNm)) and when 0% of the ballast reaction occurs in bin A (138 kip-in (15.6 kNm)) is 949 kip-in (107.2 kNm). Since bin A is the free end located the greatest distance from the rail seat load, it has the largest moment arm and the greatest effect on bending at the rail seat. The least sensitive bin for rail seat bending moment is bin C, with a difference in the 0 and 100% reactions of only -60 kip-in (-6.8 kNm). This is because it has a smaller moment arm from the rail seat.

Continuing this method of comparison to the center bending moment, bin I has the greatest sensitivity, with a difference in the 0 and 100% reactions of -1,583 kip-in (-178.9 kNm). As the reaction moves closer to the crosstie center, the distance between the rail seat load and the centroid of the reaction increases, causing greater magnitudes of negative bending. The center bending moment was found to be least affected by changes in bin D, with a difference in the 0 and 100% reactions of only 72 kip-in (8.2 kNm).

When tracking the fairly realistic case of a bin taking 25% of the ballast reaction across the crosstie (from bin A to bin I, down the 25% rows in **Table 2.1**), it is clear how quickly center negative bending moments can exceed current design recommendations. As stated by Remennikov (2007) and frequently noted by North American concrete crosstie designers, most concrete crossties are overdesigned and have reserve strength. Even so, if a crosstie was designed to meet UIC 713R, the most demanding center negative recommendation, this strength would be exceeded when bins E, F, G, H, or I take 25% or more of the ballast reaction. This shows how even small levels of center binding can potentially lead to center negative cracking.

Figure 2.2 further illustrates the change in bending moment at the crosstie center as the percent of ballast reaction in each bin changes. The maximum design bending moments found using current recommendations are also plotted to show the range in which cracking is not expected. It is easy to see

the sensitivity of each bin by the slope of its line; higher slopes indicate greater sensitivity while lower slopes indicate less sensitivity. The intersection of the lines occurs when all of the bins take the same percent of the ballast reaction. Because of the difference in bin size, this occurs when bins A-F take 13.7% and bins G-I take 5.9%.

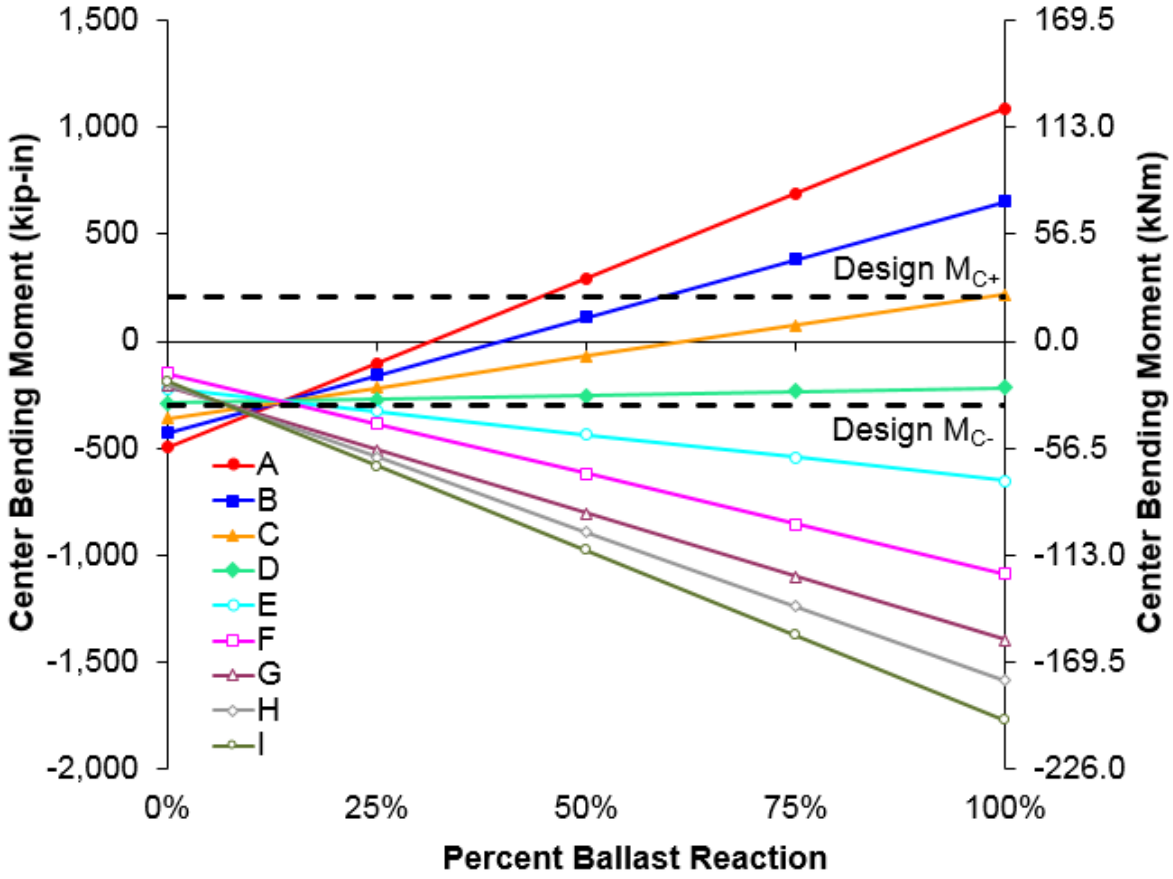

Figure 2.2 Center bending moment under changes in ballast reaction

2.4. Crosstie Bending Moments From Field-Measured Ballast Reactions

To better predict the magnitude of bending moments that could be seen in the field, support conditions found at Transportation Technology Center (TTC) (McHenry 2013) were used in the crosstie analysis model. These support conditions are shown in **Figure 2.3**. None of the zones were tamped after application of ballast, but all zones accumulated 1.5 MGT (1.36 MGT-metric) of traffic after installation.

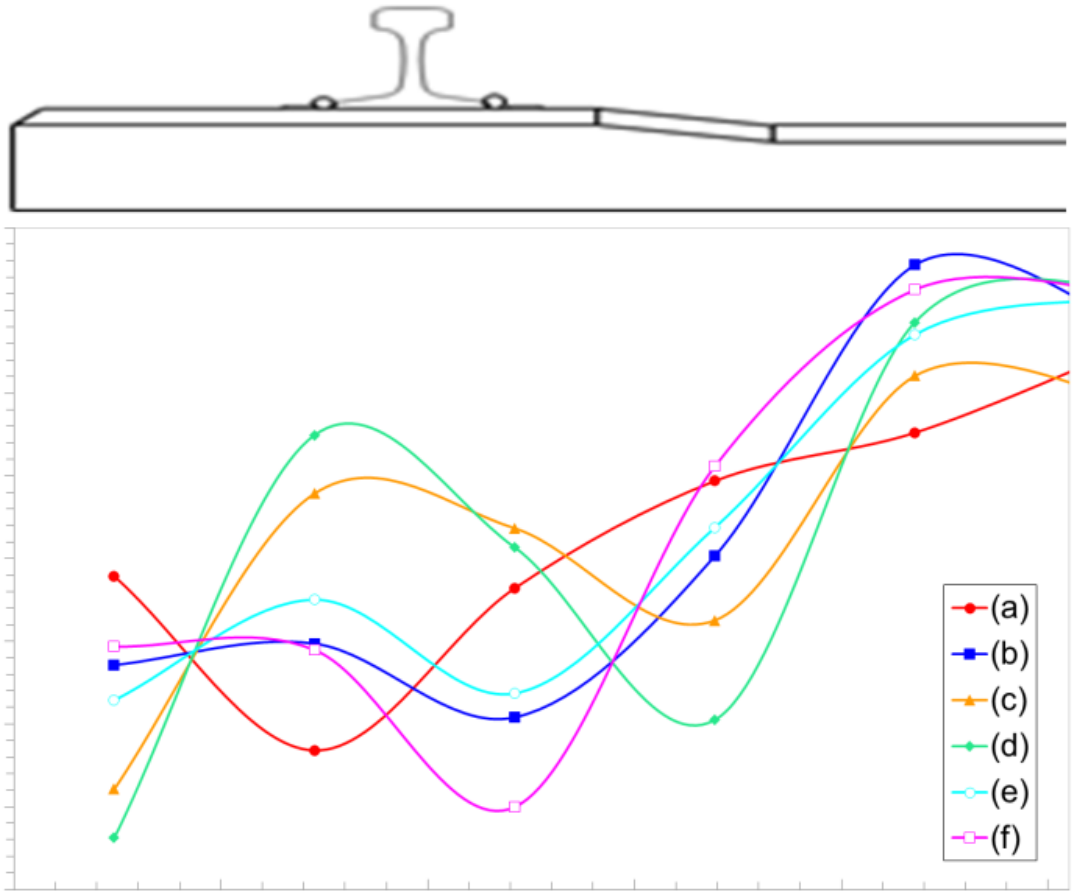

Figure 2.3 Field-measured support conditions:
(a) & (b) moderate ballast, (c) & (d) new ballast, (e) & (f) fouled ballast (McHenry 2013)

To keep the analysis consistent, the measured ballast reactions for the "heavy" train (shown in blue) were scaled to the rail seat load used in the parametric study of 62.1 kips (276.2 kN). These ballast reactions were then used in the crosstie analysis model to compute the bending moments at the rail seat and center. The results of these analyses are listed in **Table 2.2**.

Table 2.2 Theoretical bending moments for field-measured support conditions (62.1 kip (276.2 kN) rail seat load)

Crosstie	M_{RS}	M_C
Figure 2.3 (a)	364 kip-in (41.1 kNm)	105 kip-in (11.9 kNm)
Figure 2.3 (b)	308 kip-in (34.8 kNm)	-76 kip-in (-8.6 kNm)
Figure 2.3 (c)	395 kip-in (44.6 kNm)	21 kip-in (2.4 kNm)
Figure 2.3 (d)	403 kip-in (45.5 kNm)	59 kip-in (6.7 kNm)
Figure 2.3 (e)	363 kip-in (41.0 kNm)	61 kip-in (6.9 kNm)
Figure 2.3 (f)	346 kip-in (39.1 kNm)	98 kip-in (11.1 kNm)

As seen in the table above, the theoretical rail seat bending moments found using these field-measured support conditions exceeded values from all design recommendations (**Table 2.2**). In spite of this, none of the crossties were found to have experienced flexural cracking. This is most likely due to the rail seat load experienced by the crossties in this testing not reaching the 62.1 kips (276.2 kN) used in the analysis. Another possibility is that the crosstie behaved as a deep beam and transferred the rail seat load to the ballast through a compressive field (as assumed in the UIC 713R analysis), reducing the bending moment experienced at the rail seat. This theory has also been proposed by Lutch (2009).

Since the 62.1 kip (276.2 kN) rail seat load is likely on the high end of what crossties typically experience, this analysis was run again, this time with a lower, more representative rail seat load of 20 kips (89.0 kN) (Greve 2015). This can be found assuming a 40 kip (177.9 kN) wheel-rail load, which was found by Van Dyk (2014) to be near the 95th percentile of freight wheel-rail loads in North America. This wheel-rail load can then be multiplied by the 50% distribution factor (AREMA 2014) to reach 20 kips (89.0 kN). The analysis under the same support conditions yielded proportionally lower bending moments, which were below AREMA C30 limits (**Table 2.3**).

Table 2.3 Theoretical bending moments for field-measured support conditions (20 kip (89.0 kN) rail seat load)

Crosstie	M_{RS}	M_C
Figure 2.3 (a)	119 kip-in (13.5 kNm)	34 kip-in (3.9 kNm)
Figure 2.3 (b)	101 kip-in (11.4 kNm)	-25 kip-in (-2.8 kNm)
Figure 2.3 (c)	130 kip-in (14.6 kNm)	7 kip-in (0.8 kNm)
Figure 2.3 (d)	132 kip-in (14.9 kNm)	19 kip-in (2.2 kNm)
Figure 2.3 (e)	119 kip-in (13.4 kNm)	20 kip-in (2.3 kNm)
Figure 2.3 (f)	113 kip-in (12.8 kNm)	32 kip-in (3.6 kNm)

2.5. Proposed Method for Crosstie Flexural Analysis

To calculate maximum bending moments, Equations 2.2 and 2.3 are proposed. These equations are calculated with a variable center support factor (α) and a uniformly distributed rail seat load. These equations give additional transparency in assumptions and allow for easy modification to match intended maintenance practices.

$$M_{RS+} = \frac{1}{8}\left[\left(\frac{2R}{2(L-g)+\alpha(c)}\right)(L-g)^2 - Rs\right] \tag{2.2}$$

where, M_{RS+} = rail seat positive bending moment (kip-in (kNm))

R = design rail seat load (kip (kN))

L = crosstie length (in (mm))

g = rail center-to-center spacing (in (mm))

α = center support factor (-)

c = 2g-L = center support section (in (mm))

s = rail seat width (in (mm))

$$M_{C-} = \frac{1}{2} R \left[\frac{L^2 - (1-\alpha)c^2}{2(L-(1-\alpha)c)} - g \right] \quad (2.3)$$

where, M_{C-} = center negative bending moment (kip-in (kNm))

R = design rail seat load (kip (kN))

L = crosstie length (in (mm))

g = rail center-to-center spacing (in (mm))

α = center support factor (-)

c = 2g-L = center support section (in (mm))

s = rail seat width (in (mm))

Table 2.4 Recommended center support factors (α)

Crosstie Length	Center Support Factor (α)
7'-9" (2.36 m)	0.66
8'-0" (2.44 m)	0.68
8'-3" (2.51 m)	0.74
8'-6" (2.60 m)	0.84

The center support factors correspond to a 20% increase from the 2015 AREMA C30 recommendations. In the October 2015 Committee 30 meeting, these center support factors were agreed upon. In this meeting it was also agreed to the values and methodology for determining the required rail seat negative and center positive bending moments. In the 2015 AREMA recommendations the required rail seat negative bending moments were found to be equal to approximately 160 kip-in (18.1 kNm) for all crosstie lengths. This assumption was taken to be correct due to the lack of rail seat negative failures seen in the field, but it was decided to simply state this value instead of using the past factored approach. It was also found that the 2015 AREMA recommendations give a required center positive bending moment of approximately 140 kip-in (15.8 kNm) for all crosstie lengths. To make the increase in center negative bending moment more feasible and due to the lack of center positive failures seen in the field, it was

agreed that this value could be reduced to 110 kip-in (12.4 kNm). Both of these given requirements should be proportionally scaled for axle loads different than 82 kips (365 kN). Finally, for crossties longer than 8'-6" (2.60 m), the rail seat positive and center negative bending moments were set to 300 kip-in (33.9 kNm) and 200 kip-in (22.6 kNm), respectively. These values should also be proportionally scaled for axle loads different than 82 kips (365 kN). The 2015 AREMA recommended values are compared with the proposed 2017 AREMA recommended values in **Table 2.5** below.

Table 2.5 Recommended values for AREMA C30 2015 (left) and 2017 (right)

Tie Length	$\mathbf{M_{RS+}}$ kip-in (kNm)	$\mathbf{M_{RS-}}$ kip-in (kNm)	$\mathbf{M_{C-}}$ kip-in (kNm)	$\mathbf{M_{C+}}$ kip-in (kNm)	**Tie Length**	$\mathbf{M_{RS+}}$ kip-in (kNm)	$\mathbf{M_{RS-}}$ kip-in (kNm)	$\mathbf{M_{C-}}$ kip-in (kNm)	$\mathbf{M_{C+}}$ kip-in (kNm)
7'-9"	225	162	256	139	7'-9"	210	160	307	110
(2.36 m)	(25.5)	(18.4)	(29)	(15.8)	(2.36 m)	(23.7)	(18.1)	(34.7)	(12.5)
8'-0"	250	160	230	140	8'-0"	233	160	275	110
(2.44 m)	(28.3)	(18.1)	(26)	(15.9)	(2.44 m)	(26.4)	(18.1)	(31.1)	(12.5)
8'-3"	275	160	212	140	8'-3"	256	160	255	110
(2.52 m)	(31.1)	(18.1)	(24)	(15.9)	(2.52 m)	(29)	(18.1)	(28.9)	(12.5)
8'-6"	300	159	201	141	8'-6"	279	160	242	110
(2.60 m)	(33.9)	(18)	(22.8)	(16)	(2.60 m)	(31.6)	(18.1)	(27.4)	(12.5)
9'-0"	350	161	200	140	> 8'-6"	300	160	200	110
(2.74 m)	(39.6)	(18.2)	(22.6)	(15.9)	(>2.60m)	(33.9)	(18.1)	(22.6)	(12.5)

2.6. Conclusions

From this work, several conclusions relating to the flexural behavior of concrete crossties were drawn:

- The flexural behavior of a concrete crosstie is highly dependent on the crosstie support conditions. Current design recommendations make different assumptions for these crosstie support conditions, which leads to different recommended design bending moments.
- The parametric study presented shows the high level of sensitivity of the center bending moment as a function of changing support conditions. Design bending moments at the crosstie center (found in **Chapter 1**) can be exceeded under small shifts in distribution of the ballast reaction.

- Frequent tamping to keep the ballast reaction concentrated under the rail seats can prevent high center negative bending moments that cause cracking. This high sensitivity also suggests that current design recommendations for center bending moment may need to be increased.
- Crosstie span-to-depth ratios indicate that for rail seat positive bending the crosstie could behave as a deep beam, transferring load through a compressive field. As such, reductions in design bending moments for positive bending at the rail seat for both the AREMA and AS recommendations may be warranted.
- Regardless of whether a compressive field develops, treating the rail seat load as a point load is overly conservative. The assumption that the rail seat load acts over the entire width of the rail seat is used in the proposed equations.
- The support condition assumptions used in current design recommendations did not correspond closely with the support conditions measured in field testing, which suggests that current support condition assumptions may need to be modified to more closely match field conditions.

CHAPTER 3: FIELD MEASUREMENT OF BENDING MOMENTS IN PRESTRESSED CONCRETE MONOBLOCK CROSSTIES

3.1. Purpose

The purpose of this research was to measure the bending moments experienced by a concrete crosstie under typical North American freight service.

3.2. Instrumentation Technology

Researchers in the Rail Transportation and Engineering Center (RailTEC) at UIUC have selected surface-mounted strain gauges to measure the bending moments experienced by a concrete crosstie under revenue service heavy-haul freight train loads. These strain gauges were manufactured by Tokyo Sokki Kenkyujo Co, Ltd. (TML) and are specifically designed for use on concrete structural elements (Tokyo 2015). The gauge length is 1.18 in (30 mm), the gauge width is 0.1 in (2.3 mm), and the gauge resistance is 120 Ohms. Each strain gauge was plugged into a National Instruments (NI) 9235 module (NIC 2015). This module can record eight-channels of strain with each gauge placed in a quarter-bridge arrangement (i.e. one gauge per Wheatstone bridge). To capture and output the collected data on a computer, a NI compact data acquisition system (cDAQ) 9174 was used. Previous experimentation conducted by UIUC in both laboratory and field settings has implemented this instrumentation technology, and it has proven to be both cost effective and reliable (RailTEC 2013).

Prior experience has shown the importance of providing adequate protection for the strain gauges. As such, the protection plan shown in **Figure 3.1** and explained in **Table 3.1** was implemented for each strain gauge placed on the concrete crossties.

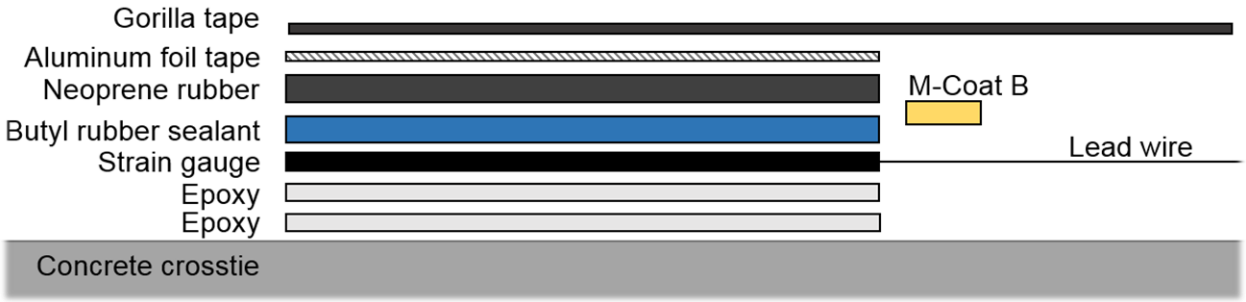

Figure 3.1 Strain gauge protection plan

Table 3.1 Explanation of strain gauge protection plan

Layer (from bottom)	Description	Purpose
Epoxy	Two-part 1 hour set time epoxy, applied in two coats: primer and secondary	Primer coat bonds with concrete surface and provides smooth surface to mount strain gauge, secondary coat bonds strain gauge to primer coat
Strain gauge	Sensor that measures change in resistance caused by small induced strains	Measures the change in strain experienced by the concrete under an applied load
Butyl rubber sealant	Sticky rubber layer	Provides moisture and mechanical protection for gauge
Neoprene rubber	Harder, stiffer rubber layer	Provides mechanical protection for gauge
Aluminum foil tape	Reflective tape layer	Provides moisture protection to gauge and holds all lower protection layers in place
Lead wire	Three-wire insulated bundled wire	Transmits strain signal recorded by gauge to data acquisition
M Coat-B	Liquid rubber sealant	Provides additional moisture protection to lead wire ends
Gorilla tape	Resilient tape layer	Provides mechanical protection to lead wire and holds all lower protection layers in place

3.3. Experimentation Plan

Field experimentation was conducted on a ballasted North American heavy-haul freight line in the western portion of the United States. Because of the high variability of support conditions seen in past experimentation (RailTEC 2013), instrumentation was placed in two locations, or "zones," of tangent track, spaced approximately 60 feet (18.3 m) apart (**Figure 3.2**). Each zone consisted of five crossties, based on the widely accepted distribution of vertical load to five crossties (Hay 1982) (**Figure 3.2**). UIUC researchers determined that the complete site of ten crossties would adequately address the need for

replicate data and encompass the variability associated with support conditions. The sampling frequency for this experimentation was set at 2,000 Hz, based on prior experience and expert recommendation.

The east zone (Zone 1) consisted of Crossties 1 – 5 and served as the example for poor support. Zone 1 was located near a group of crossties that had historically registered cross-level defects during geometry car inspections. These defects were addressed before the beginning of this experimentation, but it was believed that the issues could re-emerge. Additionally, all crossties in Zone 1 had some level of visible center negative cracking and displayed evidence of ballast pumping. The west zone (Zone 2) consisted of Crossties 6 – 10 and served as the well-supported or control zone. Crossties 6, 7, 8, and 9 showed some center cracking, but there was no visible pumping and the Zone 2 crossties deflected noticeably less than the Zone 1 crossties under train loading. Finally, there was a grade crossing located approximately 180 feet (55 meters) east of Zone 1. The track at this location consisted of 133RE rail and Safelok I fastening systems. Rail, fasteners, and crossties were all installed in 1999. As of early 2015, the track was last surfaced in an out-of-face fashion in 2011. The timetable speed at this site was 60 mph (97 kmh), the predominant direction of the traffic on this track was eastbound, and the dominant type of railcar was loaded 286 kip (129.7 tonne) coal cars.

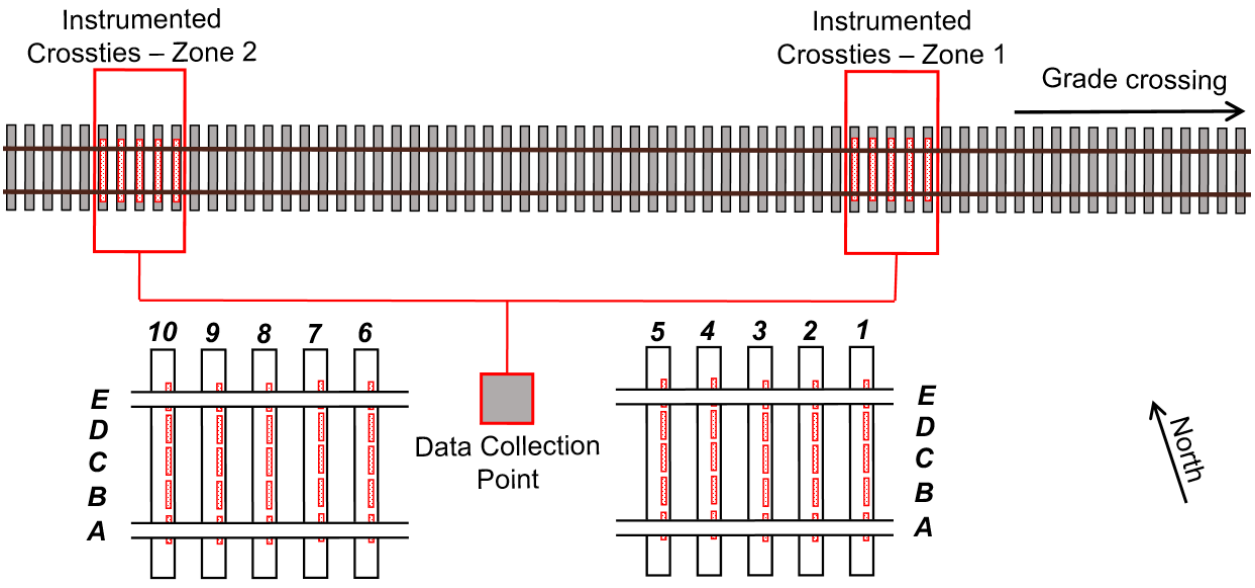

Figure 3.2 Field experimentation site layout

3.4. Instrumentation Methods

Bending strains along the length of the crosstie were measured to quantify the bending behavior of the crosstie under train loading. Surface strain gauges were applied oriented longitudinally along the chamfer near the top surface of the crosstie. A total of five strain gauges (labeled A – E) were used on each crosstie, with one at each rail seat, one at the center, and another located halfway between each rail seat and center (**Figure 3.3**).

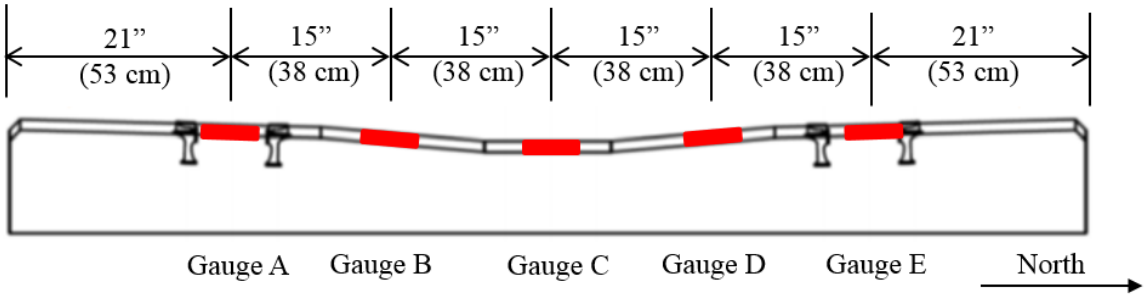

Figure 3.3 Elevation view of instrumented crosstie

To relate the measured strains to a bending moment, calibration factors were determined. This calibration factor was found by instrumenting three crossties of the same model and vintage (a representative Class I standard crosstie manufactured in 1997) as those installed in track with the strain gauge layout shown in **Figure 3.3**. The testing was performed on a loading frame at UIUC called the static tie tester (STT). The STT applies load to a crosstie using a hydraulic cylinder. These loads are monitored through a calibrated pressure gauge. Loading configurations used for these calibration tests were adapted from tests specified in Chapter 30, Section 4.9 in the AREMA MRE (AREMA 2014). Rail seat sections (Gauge A and E) were loaded in the configuration shown in **Figure 3.4a** to 40 kips (178 kN) corresponding to a moment of 255 kip-in (28.2 kNm). The gauges between the rail seat centers were loaded to 12 kips (54 kN) in the configuration shown in **Figure 3.4b**, which subjected Gauge C to a bending moment of 172.5 kip-in (19.5 kNm) and Gauge B and D to 90 kip-in (10.2 kNm).

Strain readings were then recorded on these crossties and the applied bending moment was plotted versus the measured strain. Under the applied bending moments the crossties did not experience cracking, meaning that the member remained elastic and the applied moment versus measured strain curve was

linear. As such, the calibration factor is a scalar value, and is merely the slope of the line of best fit of the moment versus strain curve. The calibration factors were 768,572.9x10^{-6} kip-in/με, 615,979.3 x10^{-6} kip-in/με, and 504,946.7 x10^{-6} kip-in/με for Gauge A and E, Gauge B and D, and Gauge C, respectively.

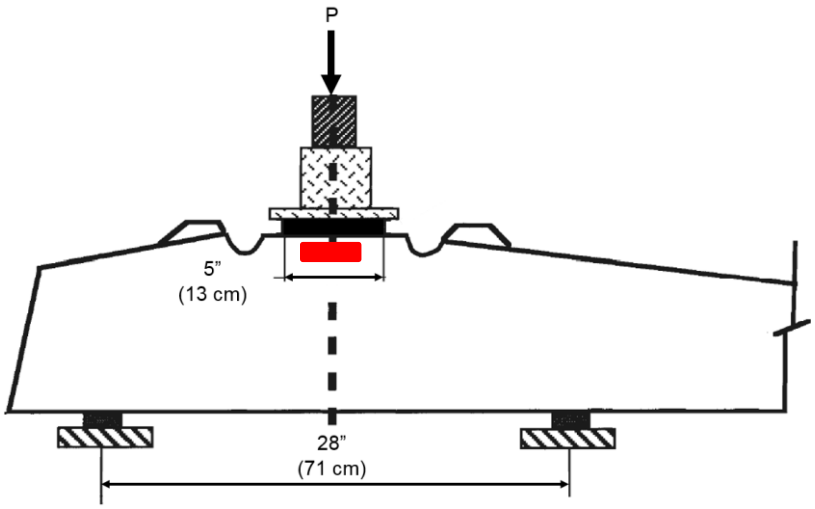

(a) Elevation view of rail seat section and loading configuration for determination of calibration factors

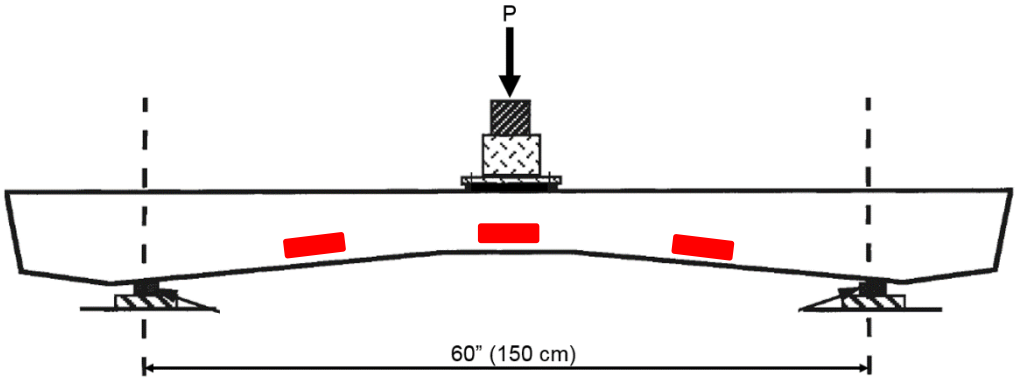

(b) Elevation view of center section and loading configuration for determination of calibration factors

Figure 3.4 Strain gauge calibration factor test configurations (adapted from AREMA 2014)

3.5. Data Analysis Procedure

To quantify the bending moments concrete crossties experience in revenue service, peaks in the strain gauge signal caused by loading of a crosstie due to an axle load must be extracted from the data stream. This was accomplished using the "findpeaks" function in MATLAB (MATLAB 2013). To improve the performance of this function for this application, several of the built-in options were utilized. To ensure that the true peaks were being captured by the program, as opposed to false peaks that did not represent

the extreme strain reading for a given axle pass, a minimum spacing ("MinPeakDistance") between the peaks was specified and a minimum value ("MinPeakHeight") for all peaks was set. To improve this process, a simple algorithm utilizing a while loop was implemented, which used the number of axles on the train as an input. The number of axles were determined using either wheel impact load detector (WILD) data, visual inspection of the passing train, or a manually-adjusted findpeaks function.

Before these peaks were obtained, the strain signal was zeroed, smoothed using a moving average filter of five data points, and the baseline was corrected to adjust for any signal drift. To aid in signal processing, data collection was started several seconds prior to the arrival of the leading axle of the first locomotive into the experimental zone. This provided a stable zero point for the crosstie under no applied load. Additionally, the data collection was ended several seconds after the passing of the final axle of the train to serve as an end point for the baseline correction. **Figure 3.5** shows an example of a typical signal for a center gauge with each peak labeled.

Each peak was then stored in a column vector with one row for each axle on the train and one column for each crosstie. In total, 7,508 loaded axles were recorded on 10 crossties at 5 locations along each crosstie from 14 train passes, for a possible 75,080 peak strains at each gauge location. Ultimately, not every peak could be resolved for each gauge location, but 73,889, 75,070, and 74,874 peaks strains were found at Gauge A, C, and E, respectively. To focus on the current design regions for concrete crossties, bending moments measured at Gauge B and D are not presented. Additionally, one train pass with unloaded railcars was measured, but these railcars failed to impart bending strains large enough to process. The outside air temperature during this testing ranged between a minimum of 36.7 °F (2.6 °C) and a maximum of 73.4 °F (23.0 °C), with an average of 61.6 °F (16.4 °C). Very light snow and light showers were experienced for a small subset of the measurements, but most of the data were recorded under overcast or clear skies. Data were collected during three site visits conducted in March, April, and May of 2015. There was a total of 0.05 (1.27 mm), 0.69 (17.53 mm), and 1.79 in (45.47 mm) of precipitation that occurred in the seven days prior to the March, April, and May visits, respectively. These data should represent bending moments in spring track conditions which has historically been considered

to be a demanding season in terms of track structure loading (Selig 1994). Currently, data are expected to be collected for 16 months, providing a means of understanding seasonal effects on the flexural performance of concrete crossties.

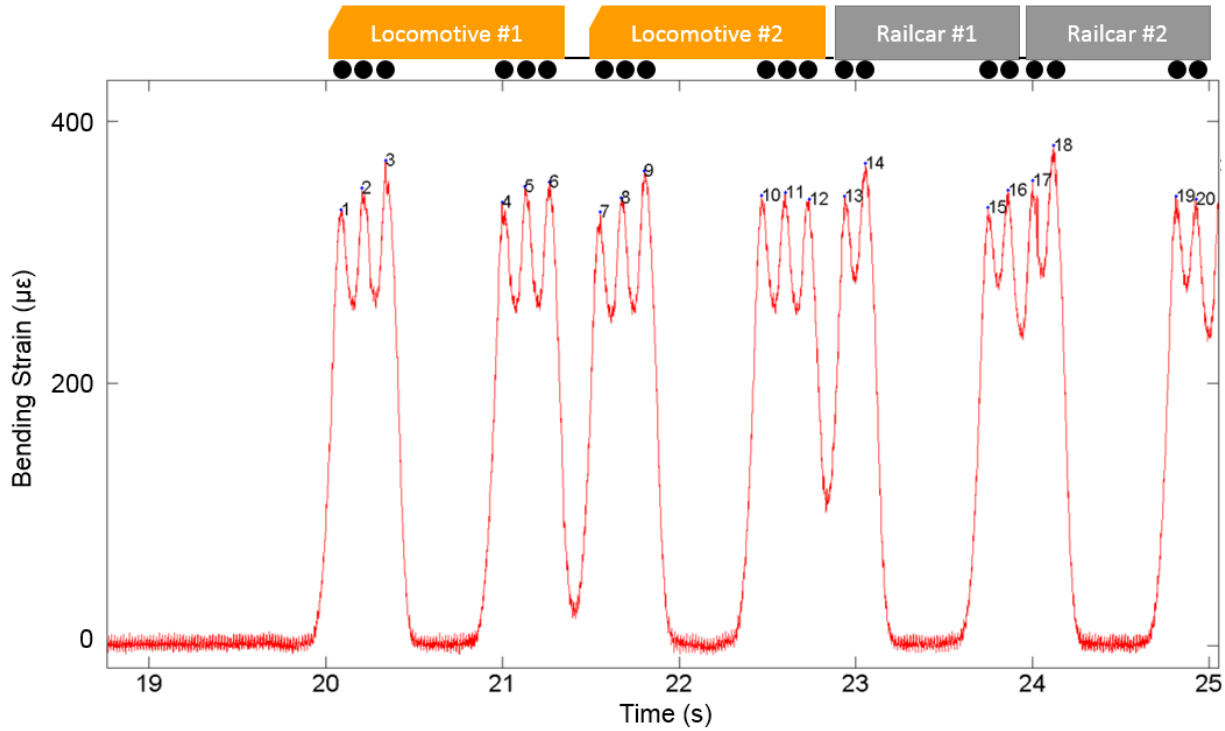

Figure 3.5 Typical strain signal captured under the passage of a loaded train

3.6. Results

3.6.1. Variation of Measured Bending Moments

To aid in the quantification of bending moments experienced by concrete crossties in North American heavy-haul freight service, peak bending moments for the site were analyzed by gauge, crosstie, and zone. One of the first observations was that the peak bending moments recorded do not follow a normal distribution. For Gauge A, C, and E, the peak bending moments for each crosstie were typically skewed to the right, with a mean larger than the median. This trend held true for both zones and over the entire site. For an individual crosstie, the computed skews were almost all greater than 0.5, indicating at least a moderate negative skew (Ott 2001). The skew decreased when analyzing a zone or the entire site, with skews closer to 0.3. For a non-normal distribution the interquartile range (IQR), found as the 75th

percentile bending moment (Q3) minus the 25th percentile bending moment (Q1), can provide an estimate of the variability of the data set – the greater the IQR, the higher the variability. Furthermore, the IQR is used to define upper and lower outliers. A concentration of data points above the mean, including some upper outliers likely caused by occasional high impact loads, cause the negative skew. An upper outlier is defined as being any data point that is greater than 1.5 times the IQR plus Q3 (or Q3 + 1.5xIQR) (Ott 2001). Similarly, a lower outlier is defined as 1.5 times the IQR minus Q1, (or Q1 - 1.5xIQR).

There were fewer outliers for Gauge C compared to Gauge A and E. Gauge C had no lower outliers and only 40 upper outliers, compared to 26 lower and 552 upper outliers and 168 lower outliers and 603 upper outliers for Gauge A and E, respectively. This is because the IQR of the center gauge was larger relative to the maximum moment than that of the rail seat gauges. This suggests that rail seat bending moments are more consistent in magnitude, but also more sensitive to flat wheels than center bending moments. The average center negative bending moment readings were higher than rail seat positive bending moment readings, and they were also more variable, with larger IQRs. In contrast, they appeared to be less sensitive to high impact loads. This agrees with prior research that found center bending to be more sensitive to support conditions than rail seat bending (**Chapter 2**).

Measured bending moments were plotted versus their percentile exceeding (**Figure 3.6**). For a given curve shown in the figure below, each point represents the percentage of loaded axles that would cause a bending moment greater than or equal to a certain magnitude. Measured bending moment curves appear to be similar to published variations of vertical wheel-rail interface loads (Van Dyk 2013) and rail seat bending moments (Dean 1980). The rail seat gauges (Gauge A and E) show the greatest similarity to the previously published data, likely because they are directly under the applied load. This also suggests that the support conditions are more uniform under the rail seat sections than the center section, as the Gauge A and E variation curves remain smooth, without the minor roughness seen in the Gauge C curve between 20% and 30% exceeding.

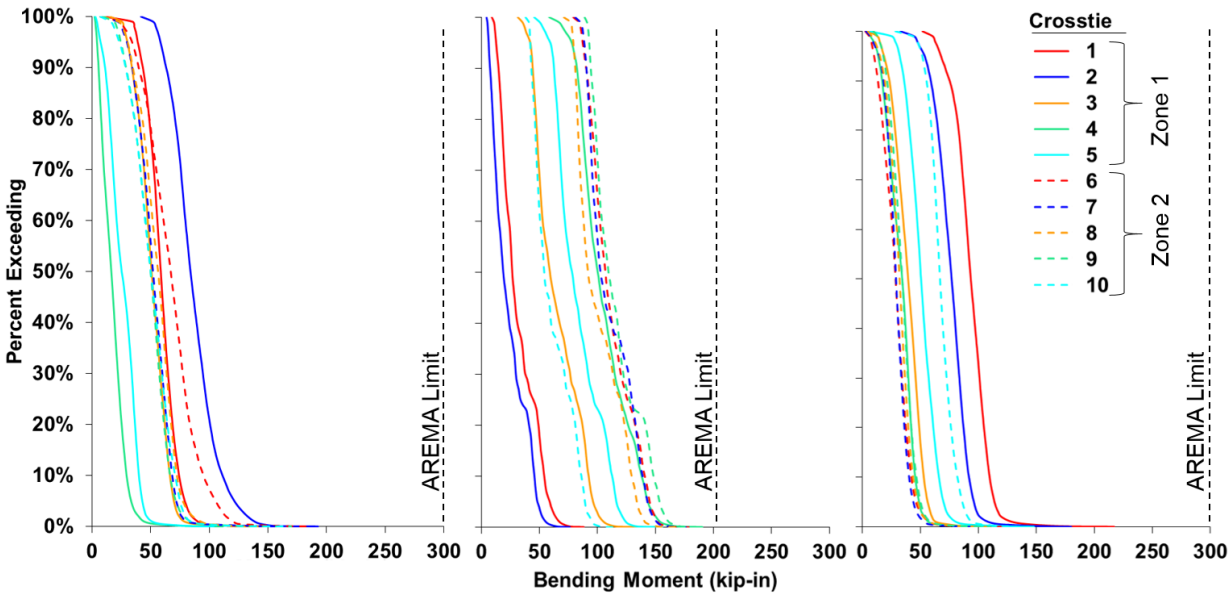

Figure 3.6 Variation of measured peak bending moments

3.6.2. Bending Strains and Moments versus Strength Limit States

When comparing the measured bending moments with the design limits set for concrete crossties in Chapter 30, Section 4.4 of the AREMA MRE (300 kip-in (33.9 kNm) for rail seat positive bending, 201 kip-in (22.7 kNm) for center negative bending), it is found that the measured bending moments fall within these limits (AREMA 2014). This suggests that cracking of the crosstie should not occur. Upon visual inspection of the crossties, this was true for the rail seat sections, but not for the center sections, as minor center cracking was seen on all crossties but Crosstie 10. The deepest these cracks were seen to propagate was approximately 0.25 inch (6.35 mm), which means that they would have to propagate another 0.75 inch (19.05 mm) to reach the top layer of prestressing steel and constitute a failure per AREMA quality control tests (AREMA 2014).

The theoretical cracking strain can be calculated using sectional properties of the crosstie. If the crosstie has an assumed compressive strength of 7 ksi (48.3 MPa) (the AREMA minimum) (AREMA 2014), 20 wires loaded to 7 kips (31.1 kN), and cross-sectional areas of 87.5 in^2 (564.5 cm^2) and 67.5 in^2 (435.5 cm^2) at the rail seat and center sections, respectively, then the cracking strain under no prestress losses can be taken to be 467 and 566 microstrain (με) at the same sections. Multiplying these theoretical

cracking strains by the measured calibration factor yields the theoretical cracking moment of the crosstie, found to be 359 kip-in (40.6 kNm) and 286 kip-in (32.3 kNm) at the rail seat and center sections, respectively. Taking into account time-dependent prestress losses due to elastic shortening of steel, creep, and shrinkage of concrete, this cracking strain decreases. Prestress losses after 15 years can be estimated to be 30% (Lutch 2009), which leads to theoretical cracking strains of 443 με (340 kip-in (38.4 kNm)) and 535 με (270 kip-in (30.5 kNm)) at the rail seat and center sections, respectively.

With these cracking thresholds in mind, the bending moments measured by Gauge C seem more significant. Crossties 4, 5, 6, 7, and 9 all experienced moments of at least 175 kip-in (19.8 kNm), with the maximum of 190 kip-in (21.5 kNm) found at Crosstie 4. While this is still 10 kip-in (1.1 kNm) from the AREMA design limits, this sample consists of 14 trains. It is possible that with effects of fatigue, vibration, center-binding, and wheel flats, this cracking limit could still be exceeded.

3.6.3. Variation of Support Conditions

Since the wheel loads experienced by each crosstie were nearly identical with the exception of the occasional higher-impact wheel load, the primary source for the difference in bending strains is assumed to be the ballast support conditions. The variability in these support conditions is evident in **Figure 3.7** where the upper whisker is the upper limit for outliers, the top line of the box is the Q3, the middle line is the median, the bottom line is the Q1, and the lower whisker is the lower limit for outliers. There is high crosstie-to-crosstie variability in support conditions, even between adjacent crossties. For example, although Crosstie 9 and 10 are adjacent to one other, the center support is different enough to cause Crosstie 9 to experience a bending moment that is nearly 60 kip-in (6.8 kNm) higher than Crosstie 10.

The support conditions were also found to be inconsistent in the transverse direction. This is seen by comparing the boxes of Gauge A and E (**Figure 3.7**). Some of the crossties, such as Crosstie 10, showed symmetric support, with similar medians for Gauge A and E. Despite these similar medians the IQR and outlier magnitudes varied greatly. More often, Gauge A and E showed different behaviors, as seen in Crosstie 4, where Gauge A's low bending moment suggests that the rail seat is poorly supported.

When comparing the bending moments along the length of each crosstie general trends can be observed. Lower rail seat positive bending moments are accompanied by higher center negative bending moments, and vice versa, following assumptions that are rooted in basic statics. The comparison between rail seat and center bending moments can indicate whether the crosstie is primarily transferring applied loads in bearing at the rail seats or in bending at the center. Using wheel load data, assumptions can be made about the rail seat loads and theoretical estimates of support conditions can be back-calculated and used to improve design recommendations.

Finally, it is important to note the difficulty in assessing support conditions from a surface-level inspection. As mentioned previously, when installing instrumentation at this site, Zone 2 was expected to be the region with less center binding and lower center negative bending moments while Zone 1 was expected to be more center bound with higher center negative bending moments. However, with a few exceptions, the initial visual assessment was shown to be incorrect. Despite signs of variable and non-ideal support such as evidence of pumping and past geometry issues, Zone 1 recorded lower center negative bending moments and higher rail seat positive bending moments, while Zone 2 recorded the opposite behavior. This could be due to the higher likelihood that Zone 1, which had seen prior geometry defects, received spot tamping at a time closer to the start of this experimentation. However, the variable support between different crossties in Zone 1 could actually be the source of these pumping and geometry issues.

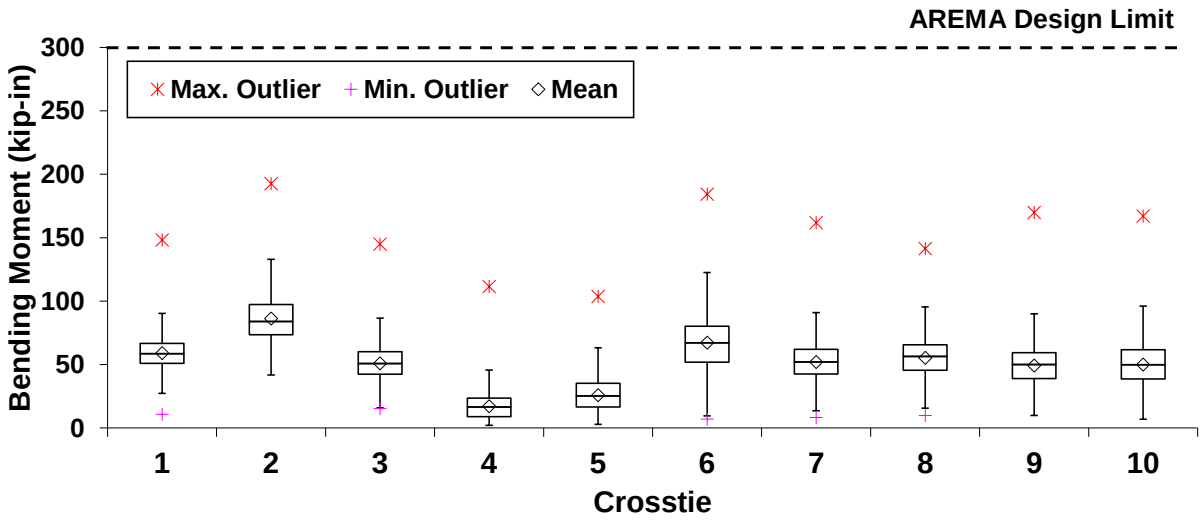

(a) Gauge A (rail seat positive bending moment)

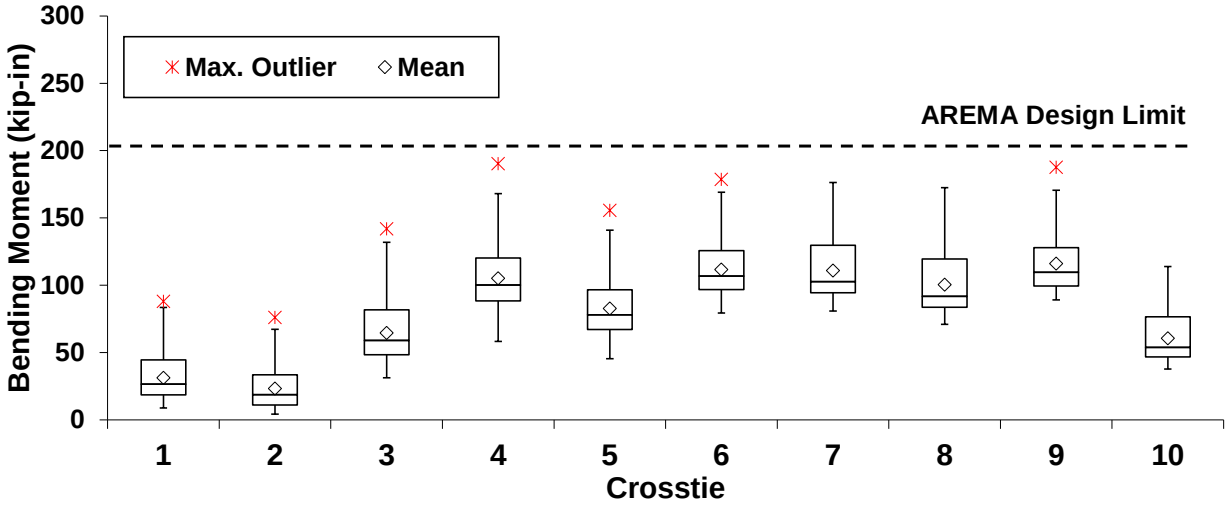

(b) Gauge C (center negative bending moment)

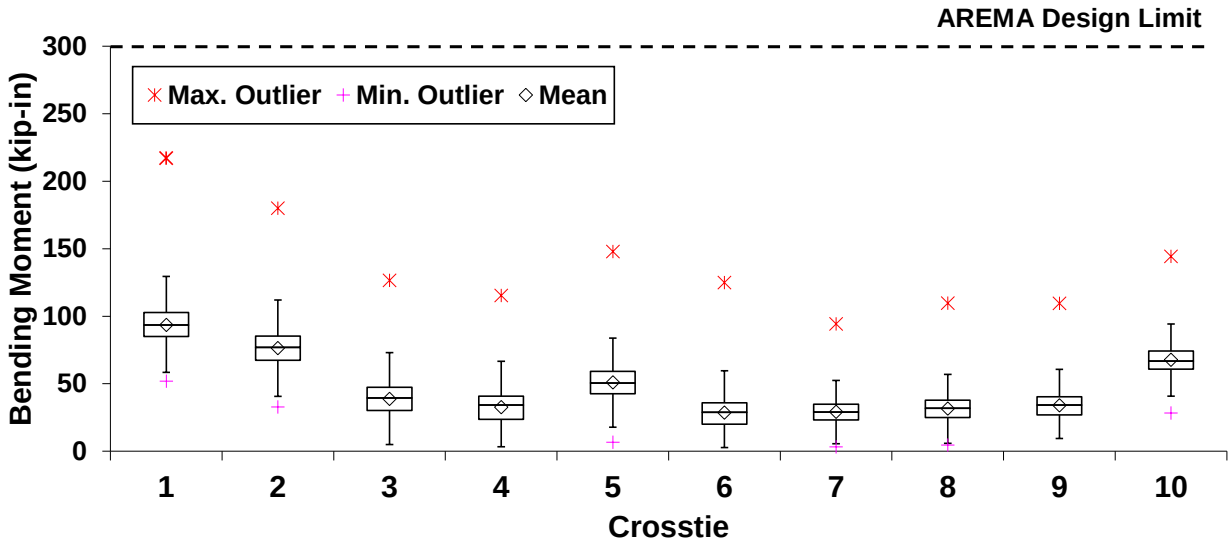

(c) Gauge E (rail seat positive bending moment)

Figure 3.7 Box-and-whisker charts of measured bending strains

3.7. Conclusions

Overall, this project was successful in measuring the bending strains and moments experienced currently in North American heavy-haul freight traffic. The effectiveness of surface-mounted concrete strain gauges in measuring crosstie bending behavior was demonstrated. From this work, several conclusions were drawn relating to the flexural behavior of concrete crossties in revenue heavy-haul freight service:

- Bending strains measured in North American heavy-haul freight traffic do not follow a normal distribution. They show moderate to significant negative skew. This skew is likely caused by upper outliers that are generated by high impact wheel loads.
- Bending strains measured at the crosstie rail seat are less variable than those experienced at the center. This could be due to more direct loading from the wheel, less sensitivity to support conditions, or more uniform support conditions under the rail seat.
- Bending moments measured at this test site did not exceed current AREMA C30 design limits, however, the instrumented crossties showed minor cracking. This could be because the cracking does not propagate to the top layer of prestressing steel, the current AREMA C30 criteria for failure of quality control tests. It should be noted that although cracking is seen on these crossties, they are performing sufficiently and have not been the source of any geometry defects since field testing began.
- Bending moments measured at this test site show a high degree of variability in support conditions. Differing bending behavior under similar wheel loading suggests that support conditions can be significantly different in both the longitudinal and transverse directions, even between adjacent crossties.

CHAPTER 4: TEMPERATURE-INDUCED CURL IN PRESTRESSED CONCRETE MONOBLOCK CROSSTIES

4.1. Purpose

The purpose of this research was to investigate whether curl occurs in concrete crossties and to better understand the implications of the behavior on crosstie flexural demand.

4.2. Introduction

Curling due to temperature gradient is a well-documented behavior in many concrete elements. Curling has been studied in concrete pavements (Armaghani 1987, Yu 1998, Rao 2005), prestressed concrete bridge girders (Imbsen 1985, Barr 2005), and concrete slab track (Zhao 2013, Song 2014), however, it has not been investigated in prestressed concrete monoblock crossties. Regardless of the element, as a temperature gradient develops the element experiences different levels of elongation along its cross-section. As seen in **Figure 4.1** below, if a concrete crosstie experiences higher temperatures on the top surface than the bottom (called a positive gradient), the top will elongate more than the bottom, causing the crosstie to curl upward. This positive gradient is usually driven by solar radiation and, as a result, is mostly experienced in the daytime (Imbsen 1985, Armaghani 1987). Conversely, if the member experiences cooler temperatures along the top and higher temperatures along the bottom (a negative gradient), the bottom will elongate more than the top and the crosstie will curl downward. Negative gradients are most likely to occur in the early morning (Armaghani 1987, Barr 2005).

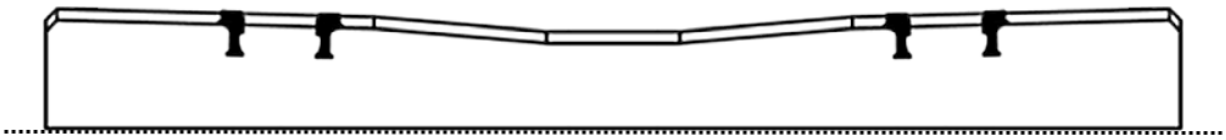

(a) Uncurled crosstie (zero gradient)

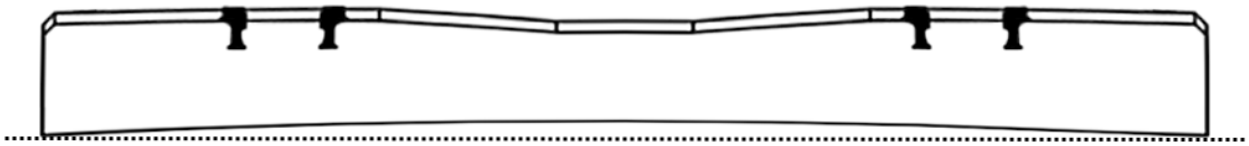

(b) Upward curl (positive gradient)

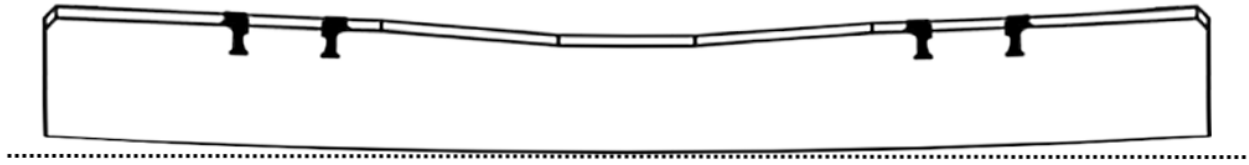

(c) Downward curl (negative gradient)

Figure 4.1 Concrete crosstie curling geometry

Curling in concrete slabs has been found to be a combination of five factors: applied temperature gradient, applied moisture gradient, built-in temperature gradient, differential drying shrinkage, and creep (Rao 2005). Temperature is the most significant of these factors, resulting in magnitudes of curl substantial enough to cause cracking and diminished mechanical performance (Armaghani 1987, Rao 2005). Armaghani (1987), Yu (1998), and Rao (2005) all measured displacements of the corner and the edge of the slab, the results of which are compiled and discussed later in this paper.

Curl, also referred to as camber (Barr 2005), due to temperature gradient has also been studied in concrete bridge girders. A comprehensive report by Imbsen (1985) compiles the findings of various research projects on thermal gradients obtained from concrete bridge superstructures. This report also compares the design practices used in different states and countries to account for temperature gradients. The report cites two ways in which temperature variation can induce stresses in concrete: temperature-caused distortions can cause internal bending moments when restrained; and nonlinear temperature gradients are prevented from causing non-linear distortion as plane sections remain plane (Imbsen 1985).

A majority of this research focused on temperature gradients in segmental box girder bridges. A study on standard prestressed, precast concrete I-beam shapes measured the temperature gradient and the deflection at midspan due these gradients (Barr 2005). This temperature-caused deflection can lead to difficulties in construction and induce stress in the superstructure (Barr 2005). The curl that was measured under these studies was compiled and is also discussed later in this paper.

4.3. Finite Element Modeling

A finite element (FE) model previously developed at UIUC (RailTEC 2013, Chen 2014) was used to perform preliminary FE simulations of crosstie curl. This 3-D model was developed using the FE software ABAQUS utilizing 8-node linear elements. The key parameters governing this curl were the coefficient of thermal expansion, specific heat, and thermal conductivity of the concrete and steel. These values were found in a literature review and are given in **Table 4.1**.

Table 4.1 Thermal Properties of FE Model

Property	Concrete	Steel
Coefficient of thermal expansion, με/°F (με/K)	5.5[a] (9.9)	6.4 (11.5)
Specific heat, 10^{-3} Btu (th)/lb-°F (J/kg-K)	239 (1000[b])	108 (452)
Thermal conductivity, Btu (th)/ in.-hr-°F (W/m-K)	0.072 (1.5[b])	2.41 (50.2)

Notes:
a – ARA, Inc. 2004, *b* – Lee 2010

The FE simulations involved applying two loading stages. The first loading stage was prestress application and transfer, the second loading stage was the application of a thermal gradient. This gradient varied in magnitude and was assumed to be linear.

The FE simulations confirmed that curl occurs in crossties (**Figure 4.2)**. **Figure 4.2** shows the crosstie in an undeformed configuration before the application of load, the crosstie after the application of prestress force, and the crosstie under a 30 °F (16.7 °C) linear temperature gradient. The curl is measured as the difference in vertical deflection at the center and at the end of the crosstie. Simulations were run for temperature gradients between -10 °F (5.6 °C) to 30 °F (16.7 °C) and the results showed that the crosstie experienced negative (downward) curl under negative and zero gradient cases and positive (upward) curl

under positive gradient cases (**Figure 4.3**). To further illustrate this behavior, the curl at a zero gradient (curl caused by prestress application) was subtracted to show only the curl caused by temperature gradient (**Figure 4.2b**).

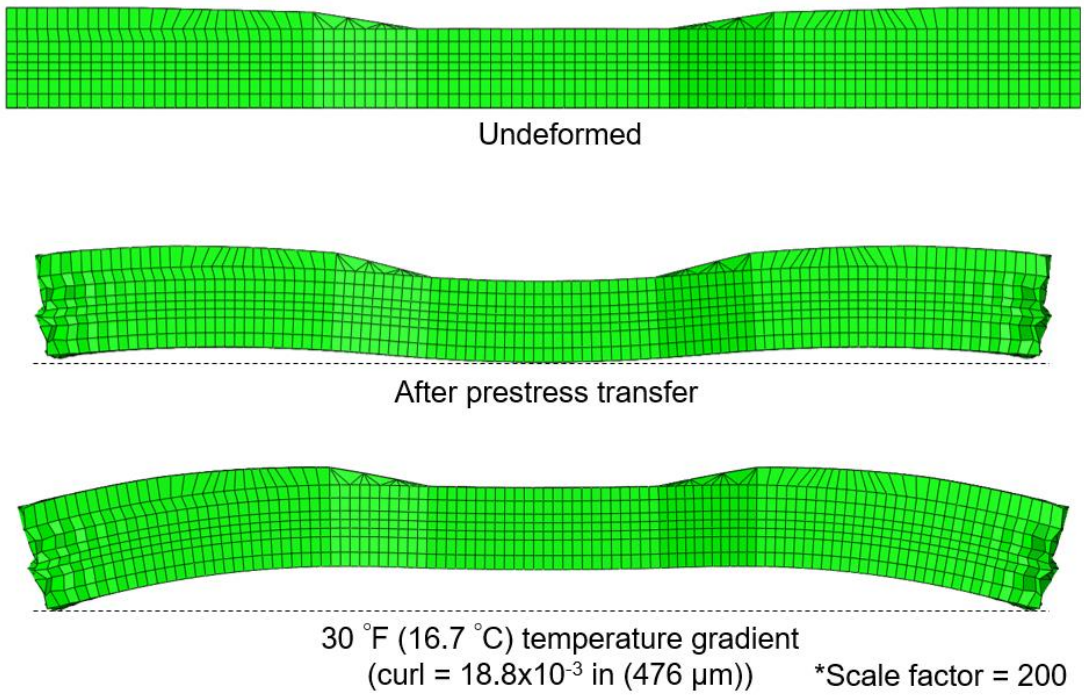

Figure 4.2 FE model curling results

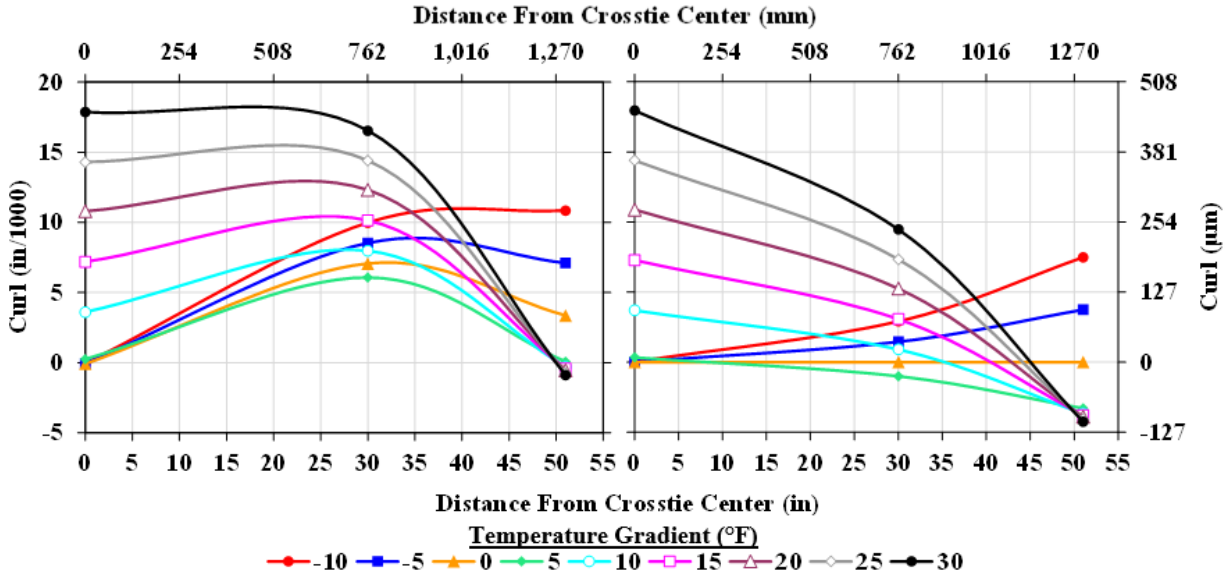

Figure 4.3 FE model curl results under varying temperature gradients (left – including prestressing effects, right – prestressing effects subtracted)

4.4. Laboratory Experimentation

Once curling was confirmed in FE simulations, laboratory experimentation was performed to quantify actual crosstie curl magnitudes. **Figure 4.4** shows a graphic of the laboratory set-up used to investigate this curling. The crosstie was first placed on 4 inches (102 mm) of premium ballast (similar to that used in the field). Special care was taken to ensure that the crosstie experienced no shade. A ballast box was built around the crosstie with approximately 12 inches (305 mm) of clearance between the crosstie and the box. Potentiometers (manufactured by NovoTechnik, model TRS-0025) were placed at each rail seat and at the center of the crosstie to measure crosstie deflection, and thermocouples (Pasco xPlorer GLX) were placed on the top, chamfer, base, and bottom of the crosstie. This box was then filled with the same type of ballast as used for the base, covering the base and bottom thermocouples. The potentiometers were plugged into a National Instruments (NI) 9205 module, with excitation provided by an NI 9237 module, both of which were placed in an NI cDAQ 9178 chasis. The thermocouples were plugged into a Pasco P-2000 system.

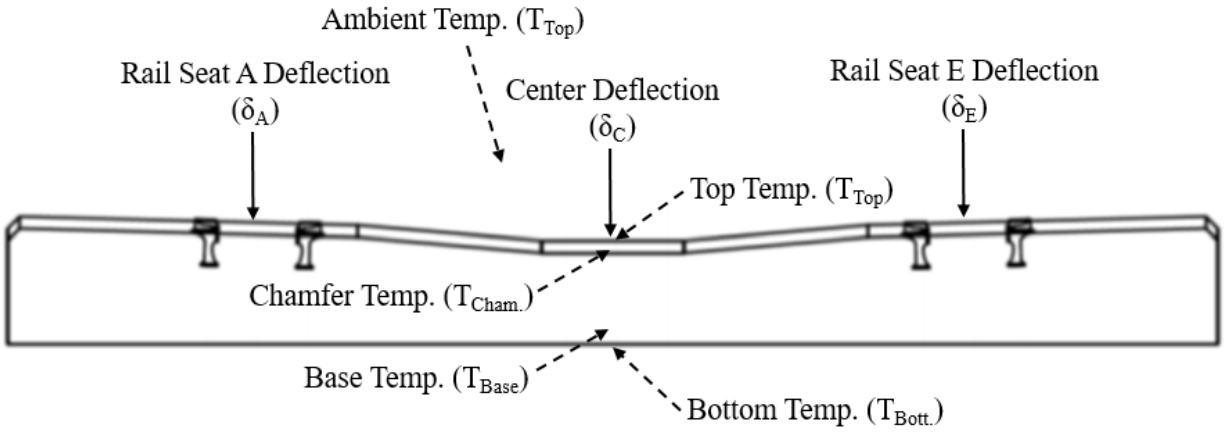

Figure 4.4 Laboratory set-up to measure temperature-induced curl

Data was collected using two systems. NI LabVIEW was used to collect data from the potentiometers and Pasco xPlorer was used to collect thermocouple data. Data points were collected once every 30 seconds, 24 hours a day, from 16:00 CST on August 3, 2015 to 16:00 CST on August 9, 2015 in Champaign, Illinois, USA.

4.5. Laboratory Results

4.5.1. Ambient Temperatures

Ambient temperatures were collected in addition to the crosstie temperatures. The full range of ambient temperatures are shown in **Figure 4.5**. Temperatures ranged from 56 °F (13 °C) to 102 °F (39 °C) with the daily high occurring between 13:30 and 15:30 and the daily low occurring between 5:00 and 6:00.

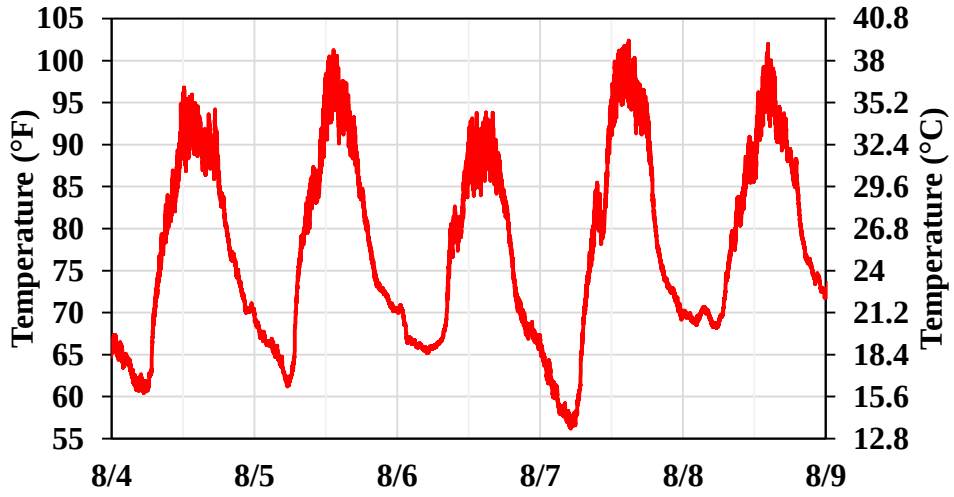

Figure 4.5 Daily fluctuations of ambient temperatures (each day marks 16:00, data recorded in August 2015)

4.5.2. Temperature Gradients

As documented in past studies, temperature gradients in concrete sections are not perfectly linear (Armaghani 1987, Yu 1998, Barr 2005). This was also seen in crosstie temperature measurements (**Figure 4.6**). Four key points of interest were extracted from the six days of data collection. These points represent the maximum positive gradient (both when comparing top and bottom temperature and chamfer and base temperatures), the maximum negative gradient when comparing top and bottom temperature, the maximum negative gradient when comparing chamfer and base temperature, and the zero gradient cases. Although these exact magnitudes were not seen every day, these general states were experienced.

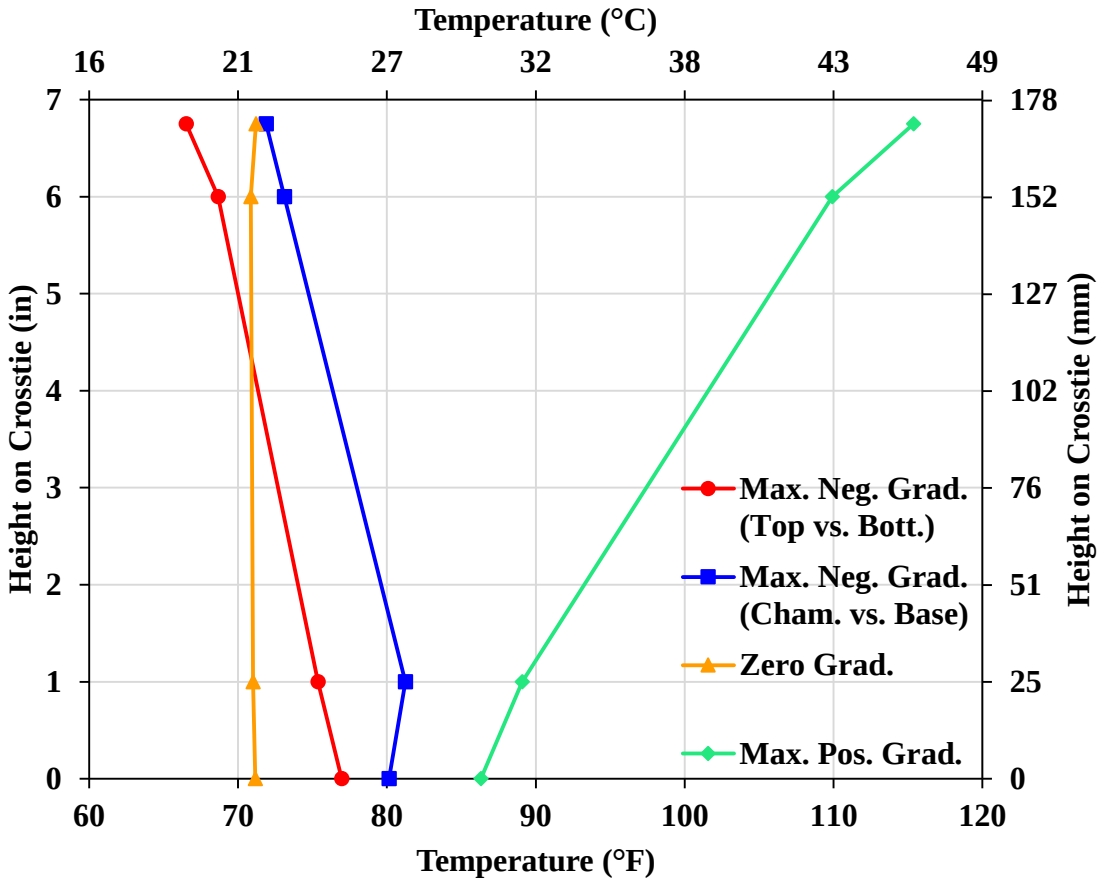

Figure 4.6 Key temperature gradients experienced during lab testing period

4.5.3. Temperature Gradients vs. Curl

The curl was calculated using Equation 4.1,

$$\text{Curl} = \delta_C - \frac{\delta_A + \delta_E}{2} \tag{4.1}$$

where δ_A, δ_C, δ_E are the measured deflections at rail seat A, crosstie center, and rail seat E, respectively (**Figure 4.3**).

The temperature gradient was found by subtracting the temperature measured at the top of the crosstie by the temperature measured at the bottom of the crosstie. It is important to note that since the data collection began and the potentiometer signals were zeroed at 16:00, the crosstie was already likely in a positive curl shape at the datum shown in **Figure 4.7**.

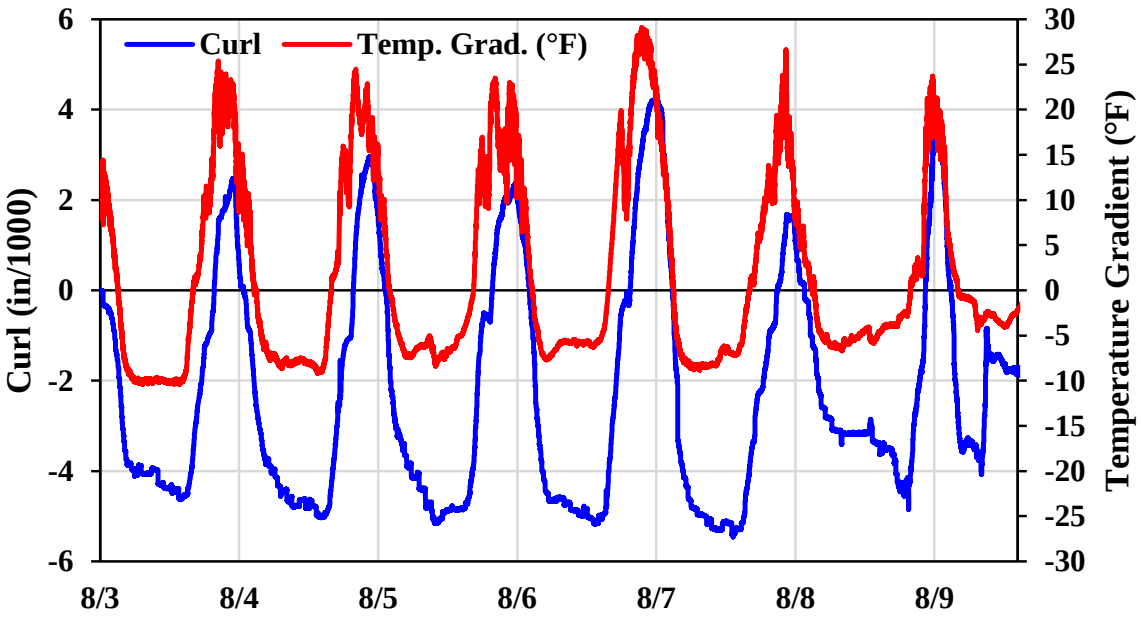

Figure 4.7 Laboratory-measured temperature-induced curl between rail seat and center (each day marks 16:00, data recorded in August 2015)

A direct relationship between curl and temperature gradient is evident in the data (**Figure 4.7**); as temperature gradient increases, curl also increases. The measured temperature gradient followed an expected cycle, increasing and reaching its maximum positive value in the mid-afternoon, then dropping down to a relatively constant maximum negative value in the early morning hours. This gradient sees some noise at high positive gradients. This noise is likely caused by intermittent cloud cover throughout the day. This noise does not significantly affect the curling of the crosstie because of the large thermal mass of the crosstie – for curling to occur, the change in temperature must occur on the entire section of the crosstie, not just the surface.

The absolute measured curl (from the highest positive curling to the lowest negative curling) was found to be 9.69 thousandths of an inch (mils) (0.25 mm). It is important to note that this curl is measured from the crosstie center to the rail seats. To make this measurement more consistent with published values in concrete slabs and bridge girders, the crosstie curl must be extrapolated to the ends of the crosstie. This can be done by assuming that the curvature of the crosstie remains constant from the rail seat centers to the ends of the crosstie. To extrapolate this curl to the crosstie ends, the measured rail seat

centers curl can be multiplied by the square of the ratio of the length of the crosstie and the distance between the rail seat centers. The length of the crosstie is 102 in (2,590 mm) and the distance between the rail seat centers is 60 in (1,524 mm), so this value is 2.89. When the measured curl is extrapolated to the crosstie ends, it yields a curl of 28 mils (0.71 mm). This can be compared with other published curl measurements, shown in **Table 4.2**.

Table 4.2 Comparison of curl in concrete crossties with pavement and girder curl

Component	Temperature Gradient, °F (°C)	Member Length, in (m)	Curl, in (mm)	Curl/Length (10^{-4})	Curvature (10^{-6}), 1/in (1/m)
Pavement[a-c]	22-34 (12-19)	120-146 (3.048-3.708)	0.039-0.07 (1-1.78)	2.67-5.83	14.6-38.9 (0.37-0.98)
Girder[d]	20 (11)	960-1644 (24.384-41.758)	0.33-0.76 (8.38-19.30)	3.44-4.62	2.3-2.9 (0.6-0.7)
Crosstie	30 (16)	102 (2.590)	0.028 (0.71)	2.75	21.5 (0.55)

Notes:
a – Armaghani 1987, *b* – Yu 1998, *c* – Rao 2005, *d* – Barr 2005

From **Table 4.2** three conclusions can be drawn. The curl measured for the crosstie was similar in magnitude to the curl measured for pavements (e.g. 0.039–0.070 in (1-1.78 mm) was comparable to 0.028 (0.71 mm) for pavements and crossties respectively). The curvature of the pavements and crosstie were also of similar magnitude (e.g. 14.6×10^{-6}-38.9×10^{-6} 1/in (0.37-0.98 1/m) was comparable to 21.5×10^{-6} 1/in (0.55 1/m) for pavements and crossties, respectively). The pavements and crosstie have similar lengths and depths, which helps to explain this similarity. And, when the curl is normalized by the member length, all components have similar values (e.g. 2.67×10^{-4}-5.83×10^{-4} for pavements, 3.44×10^{-4}-4.62×10^{-4} for girders, and 2.75×10^{-4} are all comparable).

As explained by Barr (2005) the temperature induced curl can be analytically computed with Equation 4.2. As with the FE model, the coefficient of thermal expansion was taken to be 5.5 με/°F (9.9 με/°C).

$$\text{Curl} = \frac{\sum_i \alpha_i E_i \int \Delta T_i y dA_i \, L^2}{8 \sum_i E_i I_i} \tag{4.2}$$

where, α_i = coefficient of thermal expansion

E_i = elastic modulus

T_i = temperature gradient

y = distance from neutral axis to centroid of section "i"

A_i = area of section "i"

L = length of crosstie

Equation 4.2 shows a linear relationship between curl and temperature, so the laboratory-measured curl values were plotted versus measured temperature gradient. A strong coefficient of correlation

(R^2 = 0.9776) was found using a linear trendline, given in Equation 4.3, which gives curl in mils.

$$\text{Curl} = 0.221\Delta T - 1.9068 \tag{4.3}$$

where, ΔT = temperature gradient (°F)

Figure 4.8 provides a graphical comparison between the measured curl, analytical curl, and curl computed with the trendline (empirical-linear). It is important to remember that measured curl represents the curl between the center and rail seat (i.e. this value does not include the extrapolation used in the value for crosstie curl given in **Table 4.2**). The error of the analytical curl (i.e. the difference between the analytical curl and the measured curl) was found to be between -2.11 and 3.07 mils (-54 and 78 μm) with 95% confidence. Similarly, the error of the empirical-linear curl (i.e. the difference between the empirical-linear curl and the measured curl) was found to be between -1.44 and 2.81 mils (-37 and 72 μm) with 95% confidence. Based on these results and the graphical comparison, it is seen that both Equation 4.2 (analytical curl) and Equation 4.3 (empirical-linear curl) can be used to estimate curl using temperature data.

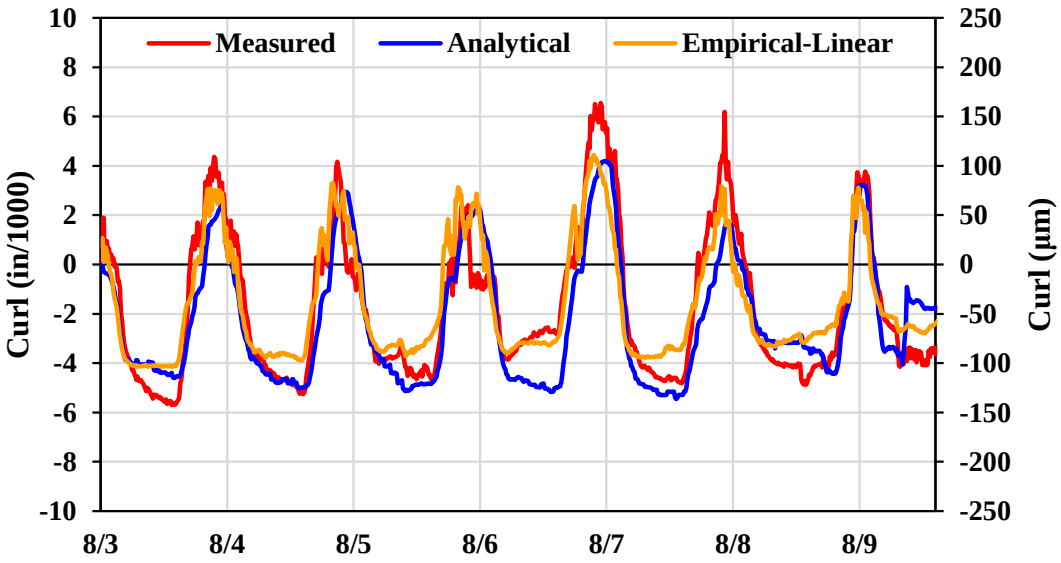

Figure 4.8 Comparison of measured and computed curl (each day marks 16:00, data recorded in August 2015)

4.6. Field Experimentation

Curl was studied as part of a larger project investigating the flexural behavior of prestressed concrete monoblock crossties. The testing site was explained in detail in **Section 3.3** of this thesis. As previously described, ten concrete crossties were instrumented with surface strain gauges in five locations along the length of the crosstie. The ten crossties were broken into two "zones" of five crossties each. Each zone had different support conditions and therefore experienced different flexural demands (**Chapter 3**). Thermocouples were placed on a crosstie located between the two zones (**Figure 4.9**).

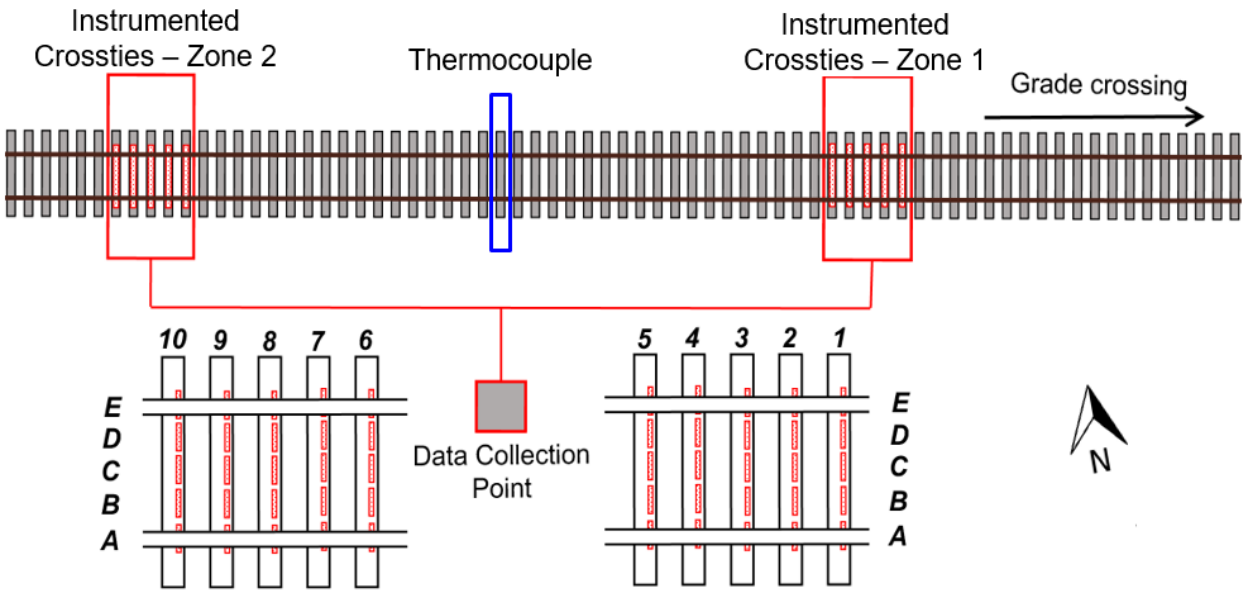

Figure 4.9 Field experimentation site layout

Bending moment and temperature gradient data were recorded during three separate site visits conducted during summer 2015 in continuation of a longer-term study. The dates, times of data collection, number of trains, and number of axles recorded each day are given in **Table 4.3**.

Table 4.3 Summary of bending moment data collected

Date	**6, 7, 8 July**	**13, 14 August**	**17 September**
No. Days	3	2	1
No. Trains	24	14	1
No. Axles	13,112	7,772	8
Time Range	0:02-21:14	8:34-19:36	7:47-15:37
Temp. Range	H: 76 °F (24 °C) L: 59 °F (15 °C)	H: 95 °F (35 °C) L: 71 °F (22 °C)	H: 97 °F (36 °C) L: 66 °F (19 °C)
Conditions	Overcast, Light drizzle	Clear	Clear

As the sun rises and the temperature gradient increases, the center negative bending moments of the crosstie decrease. This change in center negative bending moment can be attributed to curl. As seen in **Figure 4.1**, curl causes the crosstie to change shape, which in turn can alter the ballast support conditions of the crosstie. Center negative bending moments are highly sensitive to even small changes in ballast reaction at the center region (central one-third) of the crosstie (**Chapter 2**). For example, a

positive gradient would cause upward curling, which would result in a small gap forming between the ballast and the bottom of the crosstie. This gap can result in a decrease in ballast reaction at the center region, which in turn causes the center negative bending moment to decrease. The opposite of this behavior would occur under a negative gradient. The crosstie would curl downward, increasing the ballast reaction at the center region and causing an increase in center negative bending moment.

From this field experimentation, this behavior was confirmed, and it was found that the average center negative bending moment recorded changed significantly over the course of the day. **Figure 4.10** shows the strong inverse relationship between temperature gradient and center negative bending moment. This decrease can be significant in magnitude. For example, in **Figure 4.10** the average center negative bending moment of Crosstie 9 increases from 110 kip-in (12.4 kNm) to 150 kip-in (17.0 kNm) from 15:30 to 19:45, a 40 kip-in (4.5 kNm) increase. During this time, the temperature gradient changed from 20 °F (11 °C) to -4 °F (-2.2 °C). Some crossties experience even larger percentages of increase in center negative bending moment. Crosstie 2, which experiences lower center negative bending moments, sees a 30 kip-in (3.4 kNm) increase from 30 kip-in (3.4 kNm) to 60 kip-in (6.8 kNm) during the same time period. So, during a time range that saw the temperature gradient change 24 °F (13 °C), center negative bending moments for a given crosstie varied between 30 and 50%.

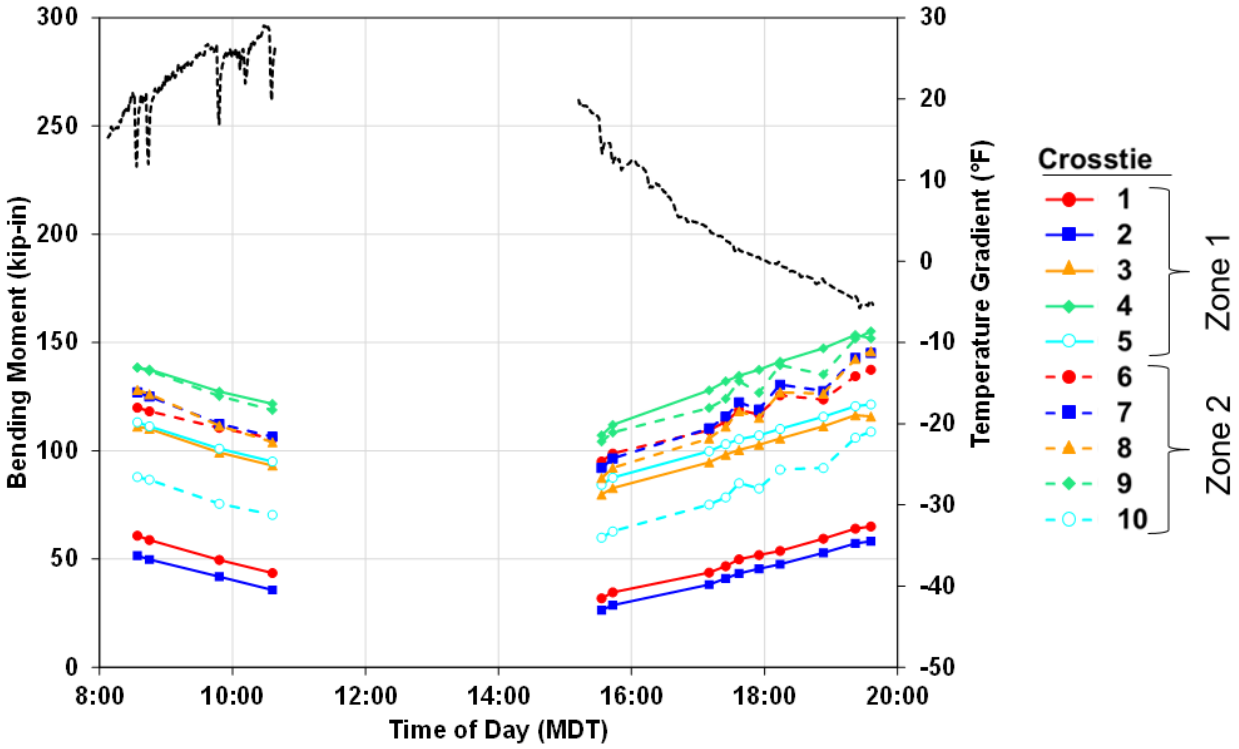

Figure 4.10 Change in average center negative bending moment over course of day

This behavior was also captured in the July and September data. In July, data were collected overnight from 0:02 to 7:54. In this timeframe, the temperature gradient varied only 1 °F (0.6 °C), ranging between -5.3 (-2.9) and -4.2 °F (-2.3 °C). In turn, the center negative bending moments remained stable, with the largest percent change recorded in any of the crossties being 5.3% (Crosstie 3 ranging between 110 kip-in (12.4 kNm) and 116 kip-in (13.1 kNm)). In September, data were collected from 7:47 to 12:02. In this timeframe, the temperature gradient increased from 10 °F (5.6 °C) to 30 °F (16.6 °C). During this time, Crosstie 2 center negative bending moments decreased from 60 kip-in (6.8 kNm) to 30 kip-in (3.4 kNm) and Crosstie 9 center negative bending center negative bending moments decreased from 160 kip-in (18.1 kNm) to 115 kip-in (13.0 kNm), a 45 kip-in (5 kNm) drop. To put the magnitude of this change into perspective, AREMA C30 recommends that a typical North American heavy-haul freight concrete crosstie have a capacity of 201 kip-in (22.7 kNm) (AREMA 2015). This means that the 45 kip-in (5 kNm) temperature-induced curl can cause changes in center negative bending moments that are nearly 25% of the total recommended capacity of the crosstie.

4.7. Conclusions

Overall, this study was successful in modeling and measuring temperature-induced curl in concrete crossties and measuring its effect on crosstie center negative bending moments. From this research, several conclusions were drawn relating to the flexural behavior of concrete crossties in revenue heavy-haul freight service:

- Curl in concrete crossties can be accurately modeled and predicted in FE simulations. Curl was shown to be directly related to temperature gradient. When prestressing effects are subtracted from crosstie curl, this relationship is even more pronounced.
- Curl in concrete crossties was seen in laboratory experimentation to change over the course of the day as the temperature gradient changed. Temperature gradients were found to fluctuate and were mostly non-linear. Laboratory-measured curl was found to be similar in magnitude to published curl values of concrete pavements. Curvature was also found be similar in pavements and crossties. Curl/length ratios of concrete pavements, girders, and crossties were all found to be similar in magnitude.
- Curl in concrete crossties can be estimated using analytical or empirical methods and measured temperature data.
- Temperature gradient and center negative bending moments have a strong inverse relationship. As temperature gradient increases, center negative bending moments decrease, and vice versa. These changes in center negative bending moment can be significant, and were measured to change center negative bending moments by as much as 45 kip-in (5 kNm) (nearly 25% of design capacity recommendations) under changes in temperature gradient of less than 30 °F (16.7 °C).

CHAPTER 5: CONCLUSIONS AND FUTURE WORK

5.1. Conclusions

The primary objective of this thesis was to improve the understanding of the flexural behavior of concrete crossties and current design recommendations. Currently, center cracking is regarded as one of the most common concrete crosstie failure mechanisms in North America. Improving the understanding of crosstie flexure can help reduce the occurrences of center cracked crossties by ensuring designs are adequate for the field conditions that are encountered. Analytical and FE methods were used to predict flexural demands and simulate bending behavior of concrete crossties. Laboratory and field experiments were also conducted to measure bending moments and deflections under real loading conditions. The following questions were addressed in the previous four chapters:

1. How are design practices used worldwide similar and different? What assumptions are made in each of these practices? (**Chapter 1**)
2. How sensitive is crosstie flexural behavior to support conditions? What are the theoretical bending moments that correspond to measured support conditions? How can this sensitivity be adjusted in a new design recommendation? (**Chapter 2**)
3. What bending moments are experienced in a representative North American heavy-haul freight line? (**Chapter 3**)
4. Does curling behavior exist in concrete crossties? How does curling affect the flexural behavior of the crosstie? (**Chapter 4**)

The following sections will summarize the primary findings related to each of these questions.

5.1.1. Comparison of Design Practices

Three international standards (AREMA C30, UIC 713R, AS 1085.14) were compared using constant design parameters. The highest values for rail seat load, center negative bending moment, and center positive bending moment bending moment were found using the UIC 713R recommendations. The highest value for rail seat positive bending moment was found using AREMA C30 and the highest value for rail seat negative bending moment was found using AS 1085.14.

In comparing the assumptions used in these analysis methodologies, two main differences were found. The first difference seen was in the assumed support conditions of the crosstie. UIC 713R and AS 1085.14 use similar support conditions for rail seat positive and center negative bending moment calculation. Both methods use a newly-tamped condition with no reaction acting at the crosstie center for calculation of rail seat positive bending and a uniform support condition with reaction acting equally along the entire length of the crosstie for center negative bending. AREMA C30 does not clearly state its support conditions, but through back-calculations, it was found that rail seat positive bending moments are found using a uniform support condition and center negative bending moments are found using a condition with a partial (61%) reaction at the center region. The second difference in design assumptions was the manner in which the rail seat load was treated. AREMA is again unclear with its assumptions on this, but it was found that the rail seat load is assumed to act as a point load at the center of the rail seat. AS 1085.14 uses the same assumption of a point load, but UIC 713R assumes that the rail seat load is distributed uniformly across the width of the rail base and spreads at a 45 degree angle to the neutral axis of the crosstie.

The review showed that AREMA C30 is not clearly based on mechanical assumptions. AREMA C30 uses the least conservative support condition assumptions between the three reviewed standards for center negative bending. As a result, its recommendation for center negative bending moments are nearly 20% less than AS 1085.14 and 40% less than UIC 713R. Increasing center negative bending moment recommendations could reduce center cracking in practice. AREMA C30 also has the highest rail seat positive bending moment recommendation of the three reviewed standards. This could help explain the lack of rail seat positive cracks seen in practice and suggest that concrete crossties are currently over-designed in the rail seat.

5.1.2. Sensitivity of Crosstie Flexure to Support Conditions

A simple analytical model was developed to conduct a sensitivity analysis of bending moments with respect to support conditions. The model assumed linear-elastic behavior and used Euler-Bernoulli beam theory. The sensitivity analysis found that crosstie flexural behavior is highly dependent on the crosstie

support conditions. Design bending moments at the crosstie center can be exceeded under small shifts in distribution of the ballast reaction. This demonstrates that the process of tamping to keep the ballast reaction concentrated under the rail seats can prevent center negative bending moments that exceed the cracking limit of the crosstie. This high sensitivity also suggests that current design recommendations for the center negative bending moment may need to be increased. Following these findings, and in conjunction with a working committee of crosstie design experts, changes to AREMA C30 are proposed. These changes result in a 20% increase in center negative bending moment compared to prior recommendations. The proposed changes are mechanistic and feature a variable center support reaction that can be easily modified to meet a railroad's maintenance practices.

5.1.3. Measurement and Quantification of Field-Measured Bending Moments

Bending moments experienced by concrete crossties under typical North American freight service were measured using surface-mounted strain gauges on three spring days. Bending moments were measured at five locations on ten crossties located in two different zones. Bending moments were found to have a non-normal distribution with negative skew. This skew was likely caused by upper outliers that are generated by high impact wheel loads. There was less variability in bending moments at the rail seat than at the center of the crosstie. Bending moments recorded at the test site did not exceed AREMA C30 design limits. Bending moments measured at this test site showed a high degree of variability in support conditions. Differing bending behavior under similar wheel loading suggests that support conditions can be significantly different in both the longitudinal and transverse directions, even between adjacent crossties. The majority of the instrumented crossties experienced higher demands in center negative bending than in rail seat positive. When this demand is compared with AREMA C30 design limits of a typical concrete crosstie it is seen that crossties are closer to exceeding their design capacities in center negative bending than rail seat positive bending. This supports the findings of the support conditions sensitivity study and the proposed changes to AREMA C30 along with explaining why center negative cracks are common in practice and rail seat positive cracks are not.

5.1.4. Curling of Concrete Crossties and Effects on Flexural Behavior

Curling due to temperature gradients is a well-documented behavior in many concrete elements (pavements, girders, and slab track), however it has not been investigated in prestressed concrete crossties. FE modeling, laboratory experimentation, and field experimentation were conducted to measure this behavior in concrete crossties. It was found that curl can be accurately modeled in FE simulations and is directly related to temperature gradient. Curl in concrete crossties was seen in laboratory experimentation to change over the course of the day as the temperature gradient changed. Temperature gradients were found to fluctuate and were mostly non-linear. Laboratory-measured curl was found to be similar in magnitude to published curl values of concrete pavements. Curvature was also found be similar in pavements and crossties. Curl/length ratios of concrete pavements, girders, and crossties were all found to be similar in magnitude. Temperature gradient and center negative bending moments have a strong inverse relationship. As temperature gradient increases, center negative bending moments decrease, and vice versa. These changes in center negative bending moment can be significant.

The implications of these findings are twofold: First, temperature data should always be collected when measuring concrete crosstie bending moments in-field. Temperature-induced curl can significantly alter support conditions and bending moments over the course of the day. Knowing the temperature gradient on the crosstie is important in fully understanding the corresponding bending moments. Second, these findings illuminate potential ways to optimize crosstie design. Upward curl on the order of 0.05 in (1.3 mm) can decrease center negative bending moments by 45 kip-in (5 kNm), nearly 25% of the design capacity at that region. Manufacturing concrete crossties with small gaps at the center region (or using under-crosstie pads at the railseat regions to create this gap) can greatly reduce center negative bending moments.

5.2. Future Work

This study has compared design standards used worldwide, shown the sensitivity of crosstie bending behavior to support conditions, quantified in-field bending moments in North American heavy-haul freight

service, and proposed changes to current AREMA C30 recommendations. Additional research is needed to improve upon these findings and key topics for future work are listed below.

5.2.1. Measure Change In Bending Moments As Tonnage Is Accumulated

The field-measured bending moments discussed in **Chapter 3** only compare the variation of data recorded in three spring months which are treated as a single dataset, independent of time and tonnage. Monitoring the change in measured bending moments as a function of tonnage could lead to improved (i.e. optimized) surfacing cycles and more informed maintenance decisions. These data can also be analyzed to investigate the differences in flexural behavior in different seasons (e.g. softer track in spring vs. stiffer track in winter).

5.2.2. Measure Effects of Surfacing on Crossties Flexural Behavior

By measuring bending moments before and after surfacing or tamping practices, the effect this maintenance has on the flexural behavior of the crosstie can be investigated.

5.2.3. Measure In-Field Bending Moments at Additional Sites in Different Locations in U.S.

The measured bending moments collected at the **Chapter 3** test site are most applicable to track experiencing similar environmental conditions. In order to broaden the understanding of concrete crosstie flexural behavior to more regions, more sites and data must be collected in more locations around North America, or internationally. Additionally, special locations of interest (e.g. poor subgrade, high moisture, distressed concrete crossties, transition zones, special trackwork, etc.) should also be instrumented to better understand the demands experienced in these locations.

REFERENCES

ABAQUS. 2014. ABAQUS/CAE 6.14, Dassault Systemes, Providence, RI.

ARA Inc., ERES Consultants Division. 2004. "Guide for Mechanistic-Empirical Design of New and Rehabilitated Pavement Structures." *NCHRP Proj. Rep. 1-37A*, Transportation Research Board, Washington, D.C.

American Railway Engineering and Maintenance-of-way Association, 2014. AREMA Manual for Railway Engineering. AREMA, Landover, Maryland.

Anon. 2008. M/W Budgets to Climb in 2008. *Railway Track and Structures* 104 (1).

Armaghani, J.M., T.J. Larsen and L.L. Smith. 1987. Temperature response of concrete pavements. *Transportation Research Record:* 23-33.

Barr, P.J., J.F. Stanton and M.O. Eberhard. 2005. Effects of temperature variations on precast, prestressed concrete bridge girders. *Journal of Bridge Engineering* 10 (2): 186–194.

Chen, Z., M. Shin, B. Andrawes and J.R. Edwards. 2014. Parametric study on damage and load demand of prestressed concrete crosstie and fastening systems. *Engineering Failure Analysis* 46: 49–61.

Dean, F.E., H.D. Harrison, J.M. Tuten, and D.R. Ahlbeck. 1980. *The Effect on Tie Pad Stiffness on the Impact Loading of Concrete Ties*. Applied Dynamics and Acoustics Section of Battelle Columbus Laboratories, Columbus, OH.

Do Carmo, T.B. 2015. Multifaceted Approach for the Analysis of Rail Pad Assembly Response. MS Thesis, Department of Civil and Environmental Engineering, University of Illinois at Urbana-Champaign, Urbana, Illinois.

European Committee for Standardization. Rail applications – Track – Concrete sleepers and bearers – Part 2: Prestressed monoblock sleepers. CEN, Brussels, Belgium.

Federation Internationale de la Precontrainte II. 1987. *Concrete Railways Sleepers - (FIP State Of Art Report)*, 1st ed. Thomos Telford Ltd.

Freudenstein, S. Concrete Ties Designed for High Dynamic Loads. Neumarkt, Germany, 2007.

Greve, M.J., M. S. Dersch, J. R. Edwards, C. P.L. Barkan, J. Mediavilla, and B. Wilson. 2014. Analysis of the Relationship between Rail Seat Load Distribution and Rail Seat Deterioration in Concrete Crossties. In Proceedings: *2014 Joint Rail Conference*, Colorado Springs, Colorado, April 2014.

Greve, M.J. 2015. Quantification of Rail Seat Load Distributions on Concrete Crossties. MS Thesis, Department of Civil and Environmental Engineering, University of Illinois at Urbana-Champaign, Urbana, Illinois.

Hay, W.W. 1982. *Railroad Engineering 2nd ed.*, John Wiley & Sons, Inc., New York, New York.

Imbsen, R.A., D.E. Vandershaf, R.A. Schamber and R.V. Nutt. 1985. "Thermal Effects In Concrete Bridge Superstructures." *NCHRP Project Report 12-22*, Transportation Research Board, Washington, D.C.

International Union of Railways, 2004. UIC 713C: Design of Monoblock Sleepers. UIC, Paris, France.

Jimenez, R. and J. LoPresti, 2004, "Performance of Alternative Tie Material under Heavy-Axle-Load Traffic," *Railway Track & Structures*, v 100, no. 1, pp. 16-18.

Kaewunruen, S. and A.M. Remennikov. 2007. Investigation of free vibrations of voided concrete sleepers in railway track system. *Journal of Rail and Rapid Transit* 221: 495-507.

Kernes, R.G. 2013. The Mechanics of Abrasion on Concrete Crosstie Rail Seats. MS Thesis, Department of Civil and Environmental Engineering, University of Illinois at Urbana-Champaign, Urbana, Illinois.

Lee, J.H. 2010. PhD Dissertation. Experimental and Analytical Investigations Of The Thermal Behavior Of Prestressed Concrete Bridge Girders Including Imperfections. Department of Civil and Environmental Engineering, Georgia Institute of Technology, Atlanta, Georgia.

Lutch, R.H. 2009. Capacity Optimization of a Prestressed Concrete Railroad Tie. MS Thesis, Department of Civil and Environmental Engineering, Michigan Technological University, Houghton, MI.

MATLAB and Signal Processing Toolbox 2013b, The MathWorks, Inc., Natick, MA.

McQueen, P.J. Flexural Performance Requirements for Prestressed Concrete Ties by Factoring. San Rafael, California, 2010.

McQueen, P.J. Introduction of Concrete Tie Systems. San Rafael, California, 1983.

National Instruments Corporation, 2015. *'NI 9235, NI 9236'*. [online], available: http://sine.ni.com/nips/cds/view/p/lang/en/nid/208790 [Accessed 13 Jun. 2015].

NovoTechnik. *'Series TR/TRS'*. [online], available: http://www.novotechnik.com/pdfs/TRTRS.pdf [Accessed 17 Nov. 2015].

Nawy, E.G. 2003. *Prestressed Concrete: A Fundamental Approach, 4th ed.* Prentice Hall, Upper Saddle River, NJ.

Ott, R.L. and M. Longnecker. 2001. *An Introduction to Statistical Methods and Data Analysis, 5th*

Pasco. 2002. *'xPlorer GLX Datalogger'*. [online], available: http://www.pasco.com/file_downloads/product_manuals/Xplorer-GLX-Manual-PS-2002.pdf [Accessed 17 Nov. 2015].

RailTEC. FRA Improved Concrete Crossties and Fastening Systems for US High Speed Passenger Rail and Joint Passenger/Freight Corridors. Railroad Transportation and Engineering Center (RailTEC), University of Illinois at Urbana-Champaign (UIUC), Urbana, Illinois, United States Department of Tranpsortation (USDOT) Federal Railroad Administration (FRA) Final Report 2013.

Rao, S. and J.R. Roesler. 2005. Characterizing effective built-in curling from concrete pavement field measurements. *Journal of Transportation Engineering* 131 (4): 320–327.

Remennikov, A.M., M.H. Murray, and S. Kaewunruen. Conversion of AS1085.14 for Prestressed Concrete Sleepers to Limit States Design Format. Wollongong, Australia, 2007.

Song, X., C. Zhao and X. Zhu. 2014. Temperature-induced deformation of CRTS II slab track and its effect on track dynamical properties. *Science China Technological Sciences* 57 (10): 1917–1924.

Standards Australia International, 2003. Australian Standard, Railway Track Material, Part 14: Prestressed Concrete Sleepers. Sydney, Australia.

Tokyo Sokki Kenkyujo Co., Ltd., 2015. '*Strain gauges|Products|Tokyo Sokki Kenkyujo Co., Ltd.'*. [online], available: http://www.tml.jp/e/product/strain_gauge/index.html [Accessed 13 Jun. 2015].

Van Dyk, B. J. 2013. Characterization of Loading Environment for Shared-Use Railway Superstructure in North America. MS Thesis, Department of Civil and Environmental Engineering, University of Illinois at Urbana-Champaign, Urbana, Illinois.

Wei, S., D.A. Kuchma, J.R. Edwards, M.S. Dersch and R.G. Kernes. 2014. Gauging Of Concrete Crossties To Investigate Load Path In Laboratory And Field Testing. In: *2014 Joint Rail Conference, JRC 2014*, Colorado Springs, Colorado, April 2014.

Wolf, H.E., J.R. Edwards, M.S. Dersch and C.P.L. Barkan. 2015. Flexural Analysis of Prestressed Concrete Monoblock Sleepers for Heavy-haul Applications: Methodologies and Sensitivity to Support Conditions. In: *Proceedings of the 11th International Heavy Haul Association Conference*, Perth, Australia, June 2015.

Zeman, J.C. 2010. Hydraulic Mechanisms of Concrete-Tie Rail Seat Deterioration. MS Thesis, Department of Civil and Environmental Engineering, University of Illinois at Urbana-Champaign, Urbana, Illinois.